Modeling and Optimization of Wastewater Treatment and Lipid Production using a Mixed-Culture of Algae and Bacteria in a High Rate Algal Pond

by

Marjan Radfar

A thesis submitted in partial fulfillment of the requirements for the degree of

Master of Science

in

Chemical Engineering

Department of Chemical and Materials Engineering

University of Alberta

Abstract

Biofuels are being considered as an alternative source of energy produced from fossil fuels. Among various biological resources, microalgae have captured lots of attention in recent years due to their potential use as renewable energy source for biofuel production since they offer high growth rate, high lipid content and potential for carbon dioxide (CO_2) capture. Cultivation of microalgae with other microorganisms in terms of promoting biomass production and other associated compounds is increasing compared to pure culture of algae. Studies on mixed culture of algae and bacteria have demonstrated the significant role of bacteria in enhancing algal growth and valuable products based on mutualistic relationship. One of the systems that is inherent in providing such medium for the interaction between algae and bacteria is high rate algal ponds (HRAPs) for wastewater treatment, with the potential for cost-effective production of biofuel. However, little attention has been devoted to study the nature of interactions from a modeling perspective. In this work, a dynamic mathematical model is presented to investigate the behavior of algal-bacterial consortium in an open pond. Wastewater serves as feed, providing substrate for bacteria and essential nutrients for the growth of algae. CO_2 is supplied into the pond as additional source of carbon for algae to grow faster and CO_2 footprint mitigation. To study the dynamic behavior of this system, the model was constituted of mass balance equations for each biological and chemical component. Gas-liquid mass transfer of CO_2 and oxygen between the atmosphere and the pond, mass transfer of the additional supplied CO_2 gas, and the effect of light intensity on algal growth were considered in the equations. The model was validated against multiple sets of experimental data in the literature and a good agreement for continuous and batch cultures was obtained. The lipid production model was incorporated into the model structure, providing reasonable predictions of the accumulated lipid in the algae for the potential generation of biofuels. The developed process model was optimized under different operating conditions to predict the

optimal paths for the combined purposes of wastewater treatment and algal growth to produce biofuel. The supplementation of CO_2 with increasing the inlet concentration of nitrogen and feeding in a stepwise pattern promoted the algal growth and lipid formation. The proposed model can be used as a tool to estimate the performance of practical algal ponds according to the desired functionality.

To my lovely parents and my sweet sister, my angel Sarah, for their unconditional love, warm support, and encouragement.

Acknowledgements

I would like to express my eternal appreciation to my supervisor, Dr. Vinay Prasad who kindly supported and inspired me during my master's program. His deep understanding, invaluable kindness and guidance allowed me to believe in my talent and strength and achieve success at this important stage of my life. It was my great honor to work under his supervision.

I am sincerely thankful to Dr. Ken Cadien for his very kind support and understanding throughout my studies. His goodness and inspiration helped me to pave the way for my success.

I gratefully acknowledge Dr. Sean Sanders for providing me with financial support. His appreciable kindness encouraged me to fulfill my educational goal at this stage.

I would like to warmly thank my dear friends Monir Hosseini, Niloofar Nayebi, Delaram Baghoori, Sepideh Kasiri, Sushmitha Thirumalaivasan, Fereshteh Sattari, Hamid Niazi, Alireza Kheradmand, Alireza Bakhtiary for their timely help and motivation in accomplishing my master's program.

Last but not least, I owe my heartfelt gratitude to my parents and my only sister for their eternal love, patience, and support throughout my life. They are the most loved ones who always do their best to sincerely support and encourage me to thrive in my life. May God bless them.

Contents

List of Tables

List of Figures

1 Introduction

Water quality issues and energy supply are the critical problems to be concerned with in the 21st century. The growing world population will require 70% increase of food, 50% increase of energy, 50% increase of water, and a 50-80% decrease in carbon dioxide (CO_2) emission to maintain political, social, and weather safety. In addition to the scarce water resources, the pollution of water has become an important environmental challenge for humanity (Salama et al., 2017) as in developing countries, this is a serious threat for people health where water supplies are being contaminated by heavy metals, organic pollutants, sewage, and acidification (Conway et al., 2015).

In terms of the energy, fossil fuels are being consumed at a fast pace and will be depleted in half a century (Panwar et al., 2011; Rawat et al., 2011). Besides the dramatic decline in fossil fuel resources, their adverse effects on the environment lead to increased health risks and global warming by carbon dioxide. The upcoming energy and environment crises have created a growing interest in developing renewable and clean resources to meet the world's high energy demands and alleviate climate changes (Panwar et al., 2011). Further, the growth of urban population results in copious generation of domestic municipal wastewater (Rawat et al., 2011). It has been reported that biomass, as a cost-effective source, is capable of producing near 25% of global energy needs in the form of biofuels, in addition to production of valuable chemicals, food additives, and pharmaceuticals (Briens et al., 2008).

To mitigate the aforementioned challenges, there has been a resurgence of interest among researchers in coupling biological wastewater treatment to bioenergy production (Salama et al., 2017). Currently, microalgae are receiving lots of attention because they can satisfy the dual purpose of wastewater bioremediation and sustainable biomass production to generate biofuel with simultaneous sequestration of carbon dioxide (Park et al., 2011; Rawat et al., 2011; Salama

et al., 2017). Furthermore, microalgae are able to proliferate in different environmental conditions and compared to other microorganisms, exhibit higher efficiency in nutrient removal since the necessary nutrients for their growth such as ammonia, nitrate, phosphate, urea and trace elements plus water are inherently available in various wastewaters (Salama et al., 2017). In fact, in the process of microalgal biofuel production, the most expensive and technically challenging stage is the microalgae mass cultivation, and therefore the integration of wastewater bioremediation and bioenergy generation brings economic and environmental advantages (Rawat et al., 2011; Salama et al., 2017). Microalgal wastewater treatment is an environment-friendly process since it allows reuse of the produced biomass and recover nutrients, avoiding secondary pollutants (Mulbry et al., 2008; Rawat et al., 2011). Figure 1-1 presents an overview of microalgae-mediated wastewater remediation with concomitant biomass generation for biofuel production. Wastewater is indigenous to many bacteria, that can compete for nutrients and be dominant because of their relatively faster growth, being a hindrance to the algae. Hence, the wastewater needs pretreatment (Figure 1-1) to eliminate competing microorganisms and decrease the suspended solids and toxicity (Salama et al., 2017).

Nowadays, it has been well established that there are bacterial species having positive effect on the algae, promoting the algal growth through the nutrient exchange (Teplitski and Rajamani, 2011). Micronutrients such as vitamins and macronutrients such as nitrogen, oxygen, and carbon are the usual ones exchanged between algae and bacteria (Fuentes et al., 2016; Teplitski and Rajamani, 2011). For example, as a result of algal-bacterial symbiosis in oxidation ponds, sewage treatment occurs based on the exchange of oxygen, carbon dioxide, and ammonium ions (Ramanan et al., 2016). In another case, co-immobilization of the algae *Chlorella vulgaris* with the growth promoter bacteria *Azospirillum brasilense* has shown an improvement in fatty acids accumulation and thus lipid formation required for biofuel production (Leyva et al., 2014).

Consequently, co-cultivation of algae with bacteria producing growth promoting factors (Fuentes et al., 2016) in a wastewater treatment process not only boosts the possibility of microalgal biomass production for biofuel generation, but also completes the wastewater bioremediation at the same time.

Different wastewaters

- Municipal wastewater
- Industrial wastewater
- Agriculture wastewater
- Piggery wastewater

Pretreatment methods

- Autoclave
- UV-radiation
- Filtration
- Dilution

Criteria for wastewater selection

- Initial nutrient concentration
- N/P ratio
- Available in industrial application

Criteria for pretreatment methods selection

- Cost-effective
- Applicable for all wastewaters
- Appropriate for large-scale

Microalgal cultivation facilities

Criteria for algal species selection

- Tolerances for wastewaters toxicity
- High growth rate with short doubling time
- High biochemical content
- Capability to grow in large-scale

Microalgal biomass

Cleaned water

- Nutrinet removal (N, P, and organic contaminants)
- Nutrients recovery
- Re-use of treated water

Biofuels

- Biohydrogen
- Bioalcohol
- Biodiesel

Figure 1-1   An overview of wastewater treatment and biofuel production by microalgae biomass cultivation (adapted from Salama et al., (2017)*)*

1.1 Thesis Outline

This thesis consists of 5 chapters focusing on the process modeling and optimization of wastewater remediation using a mixed-culture of algae and bacteria to evaluate the lipid synthesis for biofuel production. After the Introduction, Chapter 2 introduces the algae-based wastewater treatment technology developed so far and reviews the research work in terms of process modeling and simulation.

In Chapter 3, a mathematical model is developed based on the literature works associated with some changes and improvements.

Chapter 4 focuses on the results of the simulation runs and process optimization considered in this study and discusses the findings.

Lastly, Chapter 5 concludes the thesis and discusses future work.

2   Background

Microalgae can be grown in an artificial culture medium in a photobioreactor supplied with light, nutrients, and CO_2 to initiate photosynthesis. Photobioreactors can be classified into two types: open ponds and closed reactors (Borowitzka, 1999). It has been shown that closed photobioreactors can reach higher biomass productivity compared to open ponds and it is easier to control the process especially to eliminate contamination (Posten, 2009). Photobioreactors have been widely developed (Merchuk et al., 2007; Posten, 2009); however, their high capital and operating costs in comparison with open ponds cannot surpass the technical advantages of such reactors. The required nutrients and CO_2 need to be supplied from an external manufactured source in addition to light. As a result, when it comes to a practical operation especially at large scale, open ponds are the first option considered (Yang, 2011).

To make the process cost-effective to circumvent or reduce the manufactured supply of nutrients, a popular idea that has been accepted is to grow algae in a wastewater pond, rich in nutrients for cultivating algae, with CO_2 being supplied from an unwanted (waste) source such as flue gas from combustion processes (Kadam, 1997; Shilton et al., 2008; Yang, 2011). High rate algal ponds (HRAPs), first developed in the 1950s for the wastewater treatment and nutrient recovery in the form of microalgal biomass, are preferred among stabilization ponds due to their simpler design and economy (Craggs et al., 2012; Rawat et al., 2011). HRAPs are open channel, continuous raceway ponds allowing a gentle circulation of the wastewater by a paddlewheel (Craggs et al., 2012; Park et al., 2011). The water depths in these shallow ponds range from 0.2 to 1.0 m (Park et al., 2011) which accelerates photo-oxidation of dissolved organic contaminants (Craggs et al., 2012). Figure 2-1 schematically shows an HRAP with CO_2 supply.
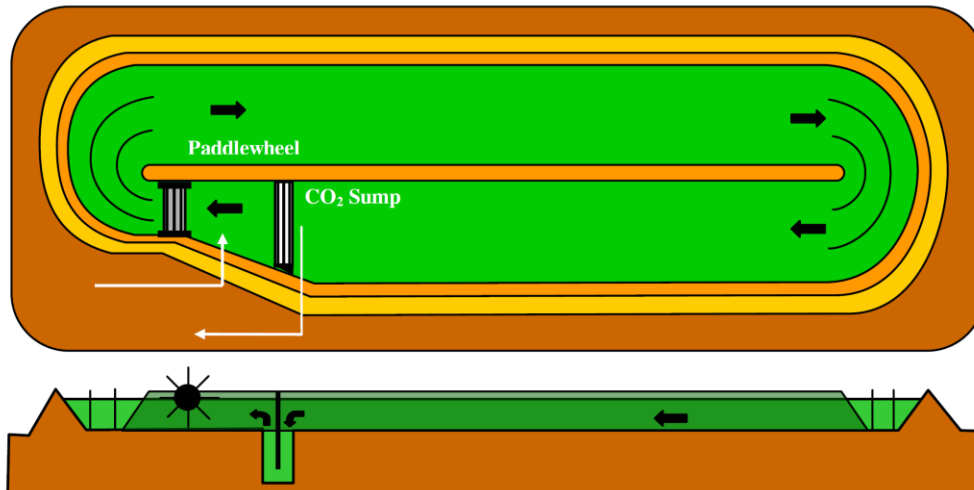
Figure 2-1   Plan and elevation view of a high rate algal pond with CO_2 injection (from Craggs et al. (2012)*)*

The main feature of HRAPs is that they provide an environment for the photoautotrophic algae and the heterotrophic bacteria to develop a symbiotic relationship (Bello et al., 2017). Compared to the conventional wastewater stabilization ponds, HRAPs have improved wastewater cleanup by growing algae and producing photosynthetic oxygen for bacterial degradation of biological oxygen demand (BOD) (Park and Craggs, 2010). Note that the removal of wastewater organic solids is measured by BOD removal (Sutherland et al., 2015). Microalgae go through photosynthesis and provide the oxygen required for aerobic bacterial breakdown of organic compounds which in turn produces the necessary CO_2 for photosynthesis (Oswald et al., 1957). This process not only saves on pond aeration energy, but also helps to mitigate the CO_2 footprint (Bordel et al., 2009). The soluble bacterial degraded organic compounds are assimilated directly by microalgae, enhancing nutrient removal through absorption into their biomass (Rawat et al., 2011); this is called the mineralization of pollutants. Therefore, the mixed culture of algae and bacteria can enhance the economic feasibility and make the microalgae biomass production effective (Bello et al., 2017).

HRAPs are carbon limited in terms of algal production because wastewaters usually have low carbon/nitrogen ratio (typically 3:1 for domestic wastewater) while this ratio is higher in algal biomass (typically 6:1) (Benemann, 2003). The rise in pond water pH during the day points out the carbon limitation as a result of inorganic carbon assimilation which shifts the carbonate system equilibrium into releasing more hydroxide ions, elevating the pH to values greater than 10 (Craggs et al., 2012). The growth of both the algae and aerobic heterotrophic bacteria are inhibited at pH>8.5 due to high concentrations of free ammonia (Azov et al., 1982). It has been reported in another study that the activity of aerobic heterotrophic bacteria is strongly inhibited at pH>8.3 (Oswald et al., 1957).

Supplementation of CO_2 has emerged as a solution to overcome the carbon source limitation in the pond, increasing the algal growth and reducing the pH (Craggs et al., 2012). This idea has been studied experimentally in several works. Azov et al. (1982) reported that when an outside pilot scale HRAP is supplied with CO_2 in addition to that transferred from the atmosphere, the algal productivity is more than twice that of a control pond without CO_2 addition. Heubeck et al. (2007) investigated the effect of CO_2 added in a HRAP used for scrubbing biogas on the performance of wastewater treatment in terms of the BOD and nutrients removal and algal production. Their results indicate enhanced wastewater nutrients recovery assimilated into the algal biomass without decrease in the wastewater treatment efficiency. Park and Craggs (2010) studied two pilot-scale HRAPs under different hydraulic retention times (HRT, 4 and 8 days) and concluded that the addition of CO_2 controlled the pond water pH to remain below 8 with up to 95% soluble organic removal and higher algal productivity was achieved in the shorter retention time. de Godos et al. (2010) evaluated the performance of two 465 L HRAPs for piggery wastewater treatment, one supplied with 7% CO_2 flue gas (2.2 and 5.5 L/min) and the other serving as a control. They stated that CO_2 input did not make remarkable changes in the removal efficiencies of organic nutrients, phosphate and ammonium ion; however, it did decrease the pH by 2 units

and boosted microalgae population, biomass production, and ammonium nitrification (higher NO_3^- and NO_2^- amounts). Consequently, CO_2 sparging is an important feature of growing algae in a wastewater treatment pond (Yang, 2011).

Coupled with the increased wastewater treatment, HRAPs offer the feature of nutrient recovery assimilated into algal biomass to be used as a feedstock for biofuel production (Benemann, 2008; Craggs et al., 2012). Compared to traditional agricultural food crops like sugar cane, soybean, canola, olive oil, maize, microalgae are desirable as a biomass source for biofuel production since they are not of concern in food security debates. Secondly, the microalgal wastewater treatment is an eco-friendly process as there is no need for chemicals such as herbicides and pesticides. Moreover, the key benefits of using microalgae are: high growth rates, ability to grow throughout the year, minimal land and water requirements, and high lipid content (Rawat et al., 2011). Capital costs for large scale cultivation of microalgae (specifically for biofuel production) are high and currently this technology is not economically viable (Benemann, 2008). However, taking advantage of the dual role of microalgae in bioremediation of the wastewater and biofuel production from their biomass makes the process economically viable since the microalgal production and harvest costs are associated with wastewater remediation costs, providing free feedstock for biofuel production (Benemann, 2003; Rawat et al., 2011). Nevertheless, the oil producing microalgae are generally unicellular and suspended, making the harvest very difficult (Moreno-Garrido, 2008). Besides that, lipid extraction methods are complicated and still being developed (Rawat et al., 2011).

Although algal-bacterium consortia has many benefits, as mentioned above, and there are a few successful full-scale plants, such a system has not been used widely due to the lack of knowledge on the design and operational parameters and management of the microalgae-based processes (Bordel et al., 2009). There are complex physicochemical and biological processes affecting the HRAP performance including: the required nutrients for algae growth, dissolved oxygen needed

for bacterial growth and oxidation of organic components, pH and temperature that control the rate of biochemical reactions, light input for photosynthesis, and hydraulic properties related to mixing in the pond (Sah et al., 2012). For a better understanding of chemical and biological interactions and improved HRAPs efficiency, a modeling-based approach has been considered as an important and low-cost tool (Bello et al., 2017; Sah et al., 2012). Reliable models help engineers to easily figure out the process performance and produce design and operational guidelines to make sure the treatment efficiencies are consistent. Only a handful of models have been developed on algal-bacterial interactions in photobioreactors and HRAP systems (Bordel et al., 2009).

The first deterministic model has been proposed by Buhr and Miller (1983) who described the symbiotic relationship of algae and bacteria in an HRAP to investigate the operational characteristics of the process and validated their model with available experimental data. They intended to consider the major features of process behavior and simulated the HRAP as a series of continuous stirred tank reactors (CSTR) with recirculation. Monod kinetics were utilized to describe the algal and bacterial growth. Jupsin et al. (2003) developed a detailed dynamic mathematical model for HRAPs using River Water Quality Model (RWQM) in which the biochemical processes are based on elemental mass balances. The model describes 21 species using ordinary differential equations (ODEs). They also considered the hydrodynamics of the system as a series of CSTRs with recirculation. Bordel et al. (2009) presented a mechanistic model for the steady-state biodegradation of an inhibitory pollutant, (salicylate) by the algal-bacterial consortium in an enclosed chemostat photobioreactor. Their modeling approach is based on stoichiometric, thermodynamic, and mass balance analysis. The model was validated against experimental data under different conditions of photon flux radiation, temperatures, HRTs, and salicylate inlet concentrations to evaluate the removal efficiency. Yang (2011) extended the model developed by Buhr and Miller (1983) to investigate the effect of CO_2 supply and utilization on the pond performance. He performed simulation studies to assess the system efficiency in terms of the algal production, wastewater remediation, and CO_2 fixation and removal under important

design and operating parameters such as pond depth, HRT, influent BOD concentration, supplied CO_2 flow rate and its fraction, and the pond bottom area used for gas sparging. Bai et al. (2015) conducted research to particularly study the contribution of bacteria on improving the algal growth experimentally and theoretically in a batch culture. They emphasized quantification of the effect of bacteria on algal productivity and considered inorganic carbon limitation in Monod kinetics. Their modeling approach is similar to but simpler than RWQM. Recently, Bello et al. (2017) developed a dynamic model based mostly on the works of Buhr and Miller (1983) and Yang (2011); however, they took a different and simpler approach in estimating the pH, only considering the chemical equilibrium-driven relation between pH and dissolved CO_2 in a functional form. Moreover, the mass transfer coefficient is assumed to be a constant value in both the exchange between the atmosphere and the pond and CO_2 induction into the pond. The mass transfer of ammonia has not been considered in their work. Their research includes studying the microalgal production under different operating conditions and sensitivity analysis of some important process parameters. They have validated their model against the experimental data of Bai et al. (2015) and the results of Solimeno et al. (2015) for a pure culture of algae in batch cultures.

2.1 Objective

The purpose of the present study was to develop a mathematical model for treatment of a generic wastewater pond mainly for lipid production and to investigate conditions that lead to higher algal growth rates and lipid accumulation. The enhanced level of lipid synthesis may improve the feasibility of biofuel production from microalgal wastewater treatment ponds and simulation can profoundly help to understand the system behavior under different operational conditions. Amongst the other models discussed above, the modeling approach used in the current work is mainly based on the model developed by Buhr and Miller (1983) as they have taken a clearer and simpler approach in considering the key interactions between the algae and bacteria. For CO_2

supply, the main concept of Yang's work (Yang, 2011) has been adopted. However, there are differences and improvements in some parts of the mentioned models related to the light function, pH estimation, and mass transfer coefficient calculation. The main feature of the current developed model is its ability to predict dynamic lipid formation within the wastewater bioremediation process. The details of the modeling work are discussed in the next chapter.

3   Model Formulation

The algal pond considered in this work is schematically represented in Figure 3-1. It is an open pond with two main inputs; sunlight and influent wastewater. The major part of the wastewater consists of biological oxygen demand (BOD), inorganic carbon species (free dissolved carbon dioxide, carbonate and bicarbonate ions), and nitrogen species (ammonia molecules and ammonium ions) (Bello et al., 2017; Buhr and Miller, 1983; Yang, 2011). It is been assumed that other nutrients including phosphorus do not act as limiting or inhibiting nutrients to the metabolism of the microbial consortium since they are available in relatively large amounts in wastewater (Bello et al., 2017; Solimeno et al., 2015; Yang, 2011). The phosphorus requirement pales in comparison to the carbon and nitrogen, and is thus neglected in the system (Buhr and Miller, 1983). The feature of gas flow injection containing CO_2 is considered in this work to understand how it affects the productivity of the system.
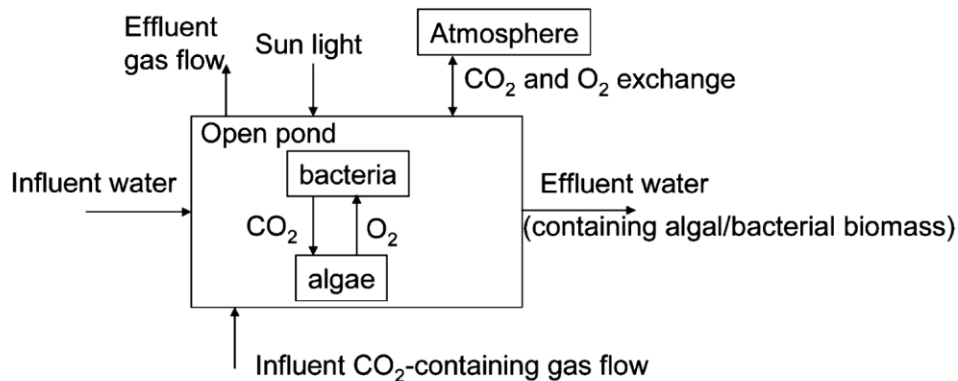
Figure 3-1   A schematic of the algal pond (from Yang (2011)*)*

There are two main outlets of the pond: effluent water, which also includes algae and bacteria biomass, and effluent flow of gas. Moreover, the mass transfer of CO_2 and oxygen (O_2) between

the pond and the atmosphere is considered and their direction of exchange depends on the amount of dissolved gases in the pond (Yang, 2011).

The pond contains a consortium of algae and bacteria. Based on their mutualistic relationship, the algae go through photosynthesis and produce oxygen which is required by the aerobic bacteria to live and grow. On the other hand, the bacteria release CO_2 that is necessary for algal metabolism (Buhr and Miller, 1983; Yang, 2011). Figure 3-2 specifically shows these interrelations including the nitrogen which is added in this work.
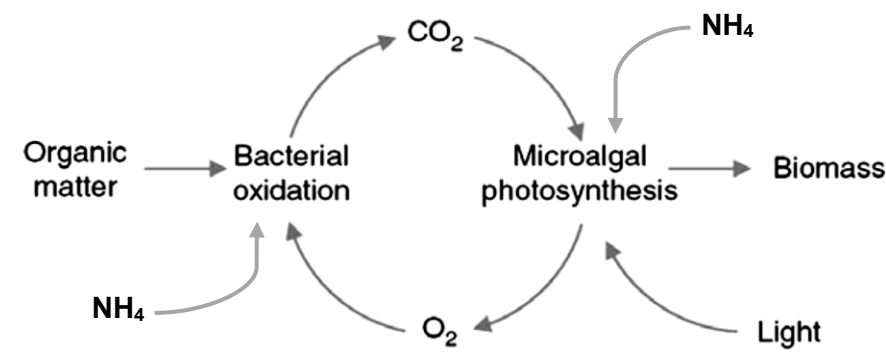
Figure 3-2   Principle of microalgae-bacteria wastewater treatment (adapted from Muñoz and Guieysse, (2006)*)*

Accounting for the interactions amongst the diverse chemical and biological components of the pond, results in a set of nonlinear differential equations obtained from the material balance for each species in the system. The entire mathematical model is discussed below.

3.1 Algal–Bacterial Consortium

The entire pond is considered as a well-mixed reactor and the behavior of the algal-bacterial consortium is investigated in a completely mixed stirred tank reactor (CSTR). In the literature (Buhr and Miller, 1983; Yang, 2011) the raceway channel of the HRAP is considered as a series of CSTRs with a recirculation flow to ensure a good mixing is provided; however, the details of the recirculation flow were not available to be included in this work. The focus of this work is mainly

on the mass balance and kinetic modeling of the algal-bacterial interactions in a wastewater treatment pond, and thus the HRAP is modeled as one CSTR.

3.1.1 Algae

The growth rate of algae is:

$$r_{gA} = \mu_A X_A \tag{3.1}$$

where μ_A and X_A are the specific growth rate (1/hr) and mass concentration of algae (g/m³), respectively. Algal specific growth rate is expressed as a function of light intensity and nutrients including dissolved carbon dioxide (CO_{2D}) and total nitrogen in a Monod-type equation (Buhr and Miller, 1983):

$$\mu_A = \mu_{Amax} \left(\frac{CO_{2D}}{K_C + CO_{2D}} \right) \left(\frac{N_T}{K_{NA} + N_T} \right) f_I \tag{3.2}$$

where μ_{Amax} is the maximum specific growth rate of algae (1/hr), K_C and K_{NA} are half-velocity constants for carbon dioxide (g CO_{2D}/m³) and total nitrogen (g N/m³). f_I is the light intensity factor expressed as Steel's function (Yang, 2011):

$$f_I = \frac{I_a}{I_s} \exp\left(1 - \frac{I_a}{I_s} \right) \tag{3.3}$$

where I_s is the saturation light intensity (MJ/m².hr) and I_a is the average light intensity in the pond (MJ/m².hr) that can be estimated using Beer-Lambert's law (Yang, 2011):

$$I_a = \frac{1}{Z}\int_0^Z I_0(t)\, exp(-K_e Z)dZ \tag{3.4}$$

where Z is the depth of pond (m) that is filled up with the liquid phase, $I_0(t)$ is the surface light intensity at a particular time point (MJ/m².hr), and K_e is the extinction coefficient. K_e is defined as (Jupsin et al., 2003):

$$K_e = K_{e1} + K_{e2}\, X_A(t) \tag{3.5}$$

K_{e1} (1/m) and K_{e2} (1/m). (m³/g) are constants. Variation of the surface light intensity during a day can be approximated by a sinusoidal function (Bello et al., 2017; Gomez et al., 2016):

$$I_0(t) = \max(0, I_0\pi(\sin(\frac{(t-6)2\pi}{24}))) \tag{3.6}$$

I_0 is the maximum surface light intensity (MJ/m².hr) during the photoperiod (assumed to be 6:00-18:00 h).

The decay rate of algae is:

$$r_{dA} = k_{dA}X_A \tag{3.7}$$

where k_{dA} is the algae decay constant (1/hr). The total mass balance of algae including the influent and effluent flow is expressed as

$$\frac{dX_A}{dt} = \frac{F}{V}(X_{Ain} - X_A) + \mu_A X_A - k_{dA}X_A \tag{3.8}$$

F is the influent and effluent flow rate (m³/hr, maintained equal to each other), V is the total volume of the reactor (m³) which contains liquid phase, and X_{Ain} is the algae concentration in the influent stream (g/m³). For a known influent flow rate, V is obtained by hydraulic retention time (HRT, 1/days) (Yang, 2011).

3.1.2 Bacteria

The growth rate of bacteria is:

$$r_{gB} = \mu_B X_B \tag{3.9}$$

where μ_B and X_B are the specific growth rate (1/hr) and mass concentration of bacteria (g/m³), respectively. The specific growth rate of bacteria can be expressed as a function of Monod-type terms to account for the limitations in organic substrate (S), oxygen (O₂), and total nitrogen (N_T) (Buhr and Miller, 1983):

$$\mu_B = \mu_{Bmax} \left(\frac{S}{K_S + S} \right) \left(\frac{O_2}{K_{O_2} + O_2} \right) \left(\frac{N_T}{K_{NB} + N_T} \right) \tag{3.10}$$

The substrate concentration is measured by BOD (Biological Oxygen Demand). μ_{Bmax} is the maximum specific growth rate of bacteria (1/hr), K_S (g BOD/m³), K_{O_2} (g O_2/m³), and K_{NB} (g N/m³) are half-velocity constants. The half-velocity constant for the nitrogen limitation does not have a known value for the bacteria reported in the literature and the same value is used for both the algae and bacteria (Bello et al., 2017; Buhr and Miller, 1983; Yang, 2011). This constant restricts the growth rate when the nitrogen depletes in the system (Buhr and Miller, 1983).

The decay rate of bacteria is expressed as:

$$r_{dB} = k_{dB} X_B \tag{3.11}$$

where k_{dB} is the bacteria decay constant (1/hr). The total mass balance of bacteria can be written in a similar way to that of algae:

$$\frac{dX_B}{dt} = \frac{F}{V}(X_{Bin} - X_B) + \mu_B X_B - k_{dB} X_B \tag{3.12}$$

X_{Bin} is the bacteria concentration in the influent stream (g/m³).

3.1.3 Substrate

The mass balance for substrate can be written as:

$$\frac{dS}{dt} = \frac{F}{V}(S_{in} - S) - \mu_B X_B Y_B \tag{3.13}$$

where S_{in} is the substrate concentration in the influent (g/m³) and Y_B is the yield of substrate consumed per mass of bacteria produced (g BOD consumed/ g bacteria produced).

3.1.4 Total Inorganic Carbon

Total inorganic carbon (TIC) is composed of dissolved carbon dioxide, carbonate and bicarbonate species.

$$TIC = CO_{2D} + [HCO_3^-] + [CO_3^{2-}] \tag{3.14}$$

The mass balance equation for total inorganic carbon is:

$$\frac{d\,TIC}{dt} = \frac{F}{V}(TIC_{in} - TIC) + \mu_B X_B Y_{BC} - \mu_A X_A Y_{AC} + f_{CO_2} - (k_l.a)_{CO_2}(CO_{2D} - CO_2^*) \tag{3.15}$$

where TIC_{in} is the influent concentration of total inorganic carbon (g/m³), Y_{BC} is the amount of CO_2 produced per mass of bacteria production (g CO_2 produced/ g bacteria produced), and Y_{AC} is the amount of CO_2 consumed per mass of algae produced (g CO_2 consumed/ g algae produced). f_{CO_2} is the flux of CO_2 gas injected into the system as the CO_2 supply flow (g/m³. hr). The last term of the above equation shows the mass transfer between the atmosphere and the pond with

$(k_l.a)_{CO_2}$ being the volumetric mass transfer coefficient (1/hr). CO_2^* is the saturation concentration of carbon dioxide in the liquid phase (g/m³) which is in equilibrium with the gaseous CO_2 and is calculated by Henry's law:

$$CO_2^* = H_{CO_2}P_{CO_2} \qquad (3.16)$$

where H_{CO_2} and P_{CO_2} are Henry's constant (g/m³.atm) and the partial pressure of CO_2 in the atmosphere (atm), respectively.

3.1.5 Oxygen

The mass balance equation for oxygen (O_2) reads:

$$\frac{dO_2}{dt} = \frac{F}{V}\left(O_{2_{in}} - O_2\right) - \mu_B X_B Y_{BO_2} + \mu_A X_A Y_{AO_2} - (k_l.a)_{O_2}(O_2 - O_2^*) \qquad (3.17)$$

where $O_{2_{in}}$ is the influent concentration of oxygen (g/m³), Y_{BO_2} is the amount of oxygen consumed per mass of bacteria produced (g O_2 consumed/ g bacteria produced), and Y_{AO_2} is the amount of produced oxygen per mass of algae production (g O_2 produced/ g algae produced). Similar to the carbon dioxide, the last term of the above equation shows the mass transfer between the atmosphere and the pond with $(k_l.a)_{O_2}$ being volumetric mass transfer coefficient (1/hr). O_2^* is the saturation concentration of oxygen in the liquid phase (g/m³) which is in equilibrium with the gaseous O_2 and is calculated by Henry's law:

$$O_2^* = H_{O_2}P_{O_2} \qquad (3.18)$$

where H_{O_2} and P_{O_2} are Henry's constant (g/m³.atm) and the partial pressure of O_2 in the atmosphere (atm), respectively.

By denoting $K_{l,O_2} = (k_l . a)_{O_2}$ and $K_{l,CO_2} = (k_l . a)_{CO_2}$, these mass transfer coefficients are estimated as (Bai et al., 2015; Yang, 2011):

$$K_{l,CO_2} = K_{l,O_2} \left(\frac{D_{CO_2}}{D_{O_2}} \right)^{1/2} \tag{3.19}$$

Where D_{CO_2} and D_{O_2} are the respective carbon dioxide and oxygen diffusion coefficients (m²/s).

3.1.6 Total Nitrogen

Nitrogen is considered as one of the limiting nutrients for the algae and bacteria. The total nitrogen (N_T) is constituted of ammonia (NH_3) and ammonium ion (NH_4^+):

$$N_T = NH_3 + NH_4^+ \tag{3.20}$$

The mass balance of N_T can be written as:

$$\frac{dN_T}{dt} = \frac{F}{V} \left(N_{T\,in} - N_T \right) - \mu_B X_B Y_{BN} - \mu_A X_A Y_{AN} - (k_l . a)_{NH_3} (NH_3) \tag{3.21}$$

where $N_{T\,in}$ is the influent concentration of total nitrogen (g/m³), Y_{BN} and Y_{AN} are yields; showing the amount of nitrogen consumed per mass of bacteria (g N consumed/ g bacteria produced) and algae produced (g N consumed/ g algae produced), respectively. Similar to the carbon dioxide and oxygen, the last term of the above equation shows the mass transfer between the atmosphere and the pond with $(k_l . a)_{NH_3}$ being the volumetric mass transfer coefficient (1/hr). The saturation concentration of ammonia (NH_3^*) is zero.

Similar to CO_2 and O_2, if $K_{l,NH_3} = (k_l . a)_{NH_3}$, it is approximated as (Yang, 2011):

$$K_{l,NH_3} = K_{l,O_2} \left(\frac{D_{NH_3}}{D_{O_2}} \right)^{1/2} \qquad (3.22)$$

D_{NH_3} represents the ammonia diffusion coefficient (m²/s).

3.1.7 Lipid Production

The Leudeking-Piret equation (Luedeking and Piret, 1959) is a widely used model to describe the kinetics of product formation. The model consists of two terms: growth and non-growth associated phenomena which are linearly connected to cell concentration and their growth rate (Surendhiran et al., 2015; Tevatia et al., 2012; Yang et al., 2011a):

$$\frac{dP}{dt} = \alpha \frac{dX}{dt} + \beta X \qquad (3.23)$$

where P(t) is concentration of the produced lipid (g/m³), α is the lipid formation coefficient (g/g), and β is the non-growth correlation coefficient (g/g.hr) (Tevatia et al., 2012; Yang et al., 2011b). The model parameters, α and β are variable and dependent to the process dynamics (Surendhiran et al., 2015).

Gaden (1959) described product formation states in three classes: in Class I, the product is produced in a direct relationship with the cell growth ($\alpha \neq 0$ and $\beta = 0$); in Class II, the product formation is partially related to the cell growth ($\alpha \neq 0$ and $\beta \neq 0$); and Class III defines the product formation as an unrelated process to the cell growth ($\alpha = 0$ and $\beta \neq 0$). In this work, lipid formation kinetics are considered under the class II based on the literature (Surendhiran et al., 2015; Tevatia et al., 2012).

To determine the lipid production from algae in the pond in a continuous system, the mass balance equation can be expressed as:

$$\frac{dP}{dt} = \frac{F}{V}(P_{in} - P) + \alpha \frac{dX_A}{dt} + \beta X_A \tag{3.24}$$

where P_{in} is the amount of lipid in the influent flow (g/m³). For estimating α and β, the previous researchers have reported model fit parameters according to their own measured experimental data (Surendhiran et al., 2015; Tevatia et al., 2012; Yang et al., 2011b). Tevatia et al. (2012) have proposed fitted equations based on experimental data for these coefficients as a function of ammonium ion concentration (mol/m³). Their correlations are adopted in this work and allow dynamic prediction of the coefficients based on the available nutrient (the ammonium ion amount in this case). The equations are:

$$\alpha = -(8 \times 10^{-5})[NH_4^+]^2 + 0.0023[NH_4^+] - 0.013 \tag{3.25}$$

$$\beta = (4 \times 10^{-6})[NH_4^+]^2 - (9 \times 10^{-5})[NH_4^+] + (4 \times 10^{-4}) \tag{3.26}$$

3.1.8 pH Estimation

The interrelationships among the ammonium, inorganic carbon species, and other non-reacting ions in an aquatic system are well documented and the pH estimation method in this work is based on solution equilibrium and charge neutrality principles (Loewenthal and Marais, 1976). The pH model used here is similar to that of Buhr and Miller (1983); however, unit activity coefficient is considered, making the estimation simpler. The model takes into account dynamic pH changes, which is important in dissolved carbon dioxide estimation and determines it while including both the total nitrogen and inorganic carbon.

Ammonia stays in an equilibrium state with ammonium ion in water (Bates and Pinching, 1949):

$$NH_3 + H_2O \overset{K_B}{\Leftrightarrow} NH_4^+ + OH^- \tag{3.27}$$

K_B is the basic dissociation constant of ammonia (molar units) and is related to the acidic

dissociation constant, K_A by $K_B = \frac{K_W}{K_A}$ in which K_W is the water dissociation constant. K_B is defined

as:

$$K_B = \frac{[NH_4^+][OH^-]}{NH_3} \tag{3.28}$$

The concentration of the ammonia ion (mol/m³) can be written as (Buhr and Miller, 1983):

$$[NH_4^+] = \frac{(N_T)[H^+]}{K_A + [H^+]} \tag{3.29}$$

The carbonic species in water forms a state of dynamic equilibrium based on the following

reactions:

$$CO_{2(aq)} + H_2O \Leftrightarrow H_2CO_3 \tag{3.30}$$

$$H_2CO_3 \Leftrightarrow H^+ + HCO_3^- \tag{3.31}$$

$$HCO_3^- \Leftrightarrow H^+ + CO_3^{2-} \tag{3.32}$$

$$H_2O \Leftrightarrow H^+ + OH^- \tag{3.33}$$

For the first two reactions, the dissociation equation is expressed as:

$$\frac{[H^+][HCO_3^-]}{CO_{2(aq)}} = K_1 \tag{3.34}$$

The second dissociation constant for the dissociation of HCO_3^- is:

$$\frac{[H^+][CO_3^{2-}]}{[HCO_3^-]} = K_2 \tag{3.35}$$

The dissociation equation of water is:

$$[H^+][OH^-] = K_w \tag{3.36}$$

Based on the principle of electro-neutrality and considering the presence of inert cations and anions:

$$[NH_4^+] + [H^+] + [inert\ cations] = [HCO_3^-] + 2[CO_3^{2-}] + [OH^-] + [inert\ anions] \tag{3.37}$$

$$inert = [inert\ cations] - [inert\ anions] \tag{3.38}$$

$inert$ includes inert ions other than $NH_4^+, HCO_3^-, CO_3^{2-}, OH^-, and\ H^+$ (Buhr and Miller, 1983; Yang, 2011).

Rearranging equation (3.37) gives:

$$[NH_4^+] + inert = [HCO_3^-] + 2[CO_3^{2-}] + [OH^-] - [H^+] \tag{3.39}$$

Substituting for $[CO_3^{2-}]$ from equation (3.35) into (3.39) and solving for $[HCO_3^-]$:

$$[HCO_3^-] = \frac{[NH_4^+] + inert - [OH^-] + [H^+]}{(1 + 2K_2/[H^+])} \tag{3.40}$$

Substituting for $[HCO_3^-]$ from equation (3.40) into equation (3.34) and solving for $CO_{2(aq)}$:

$$CO_{2(aq)} = \frac{[NH_4^+] + inert - [OH^-] + [H^+]}{\left(\dfrac{K_1}{[H^+]} + \dfrac{2K_2K_1}{[H^+]^2}\right)} \tag{3.41}$$

Furthermore, substituting for $[HCO_3^-]$ from equation (3.40) into equation (3.35) and solving for $[CO_3^{2-}]$ gives:

$$[CO_3^{2-}] = \frac{[NH_4^+] + inert - [OH^-] + [H^+]}{\left(\dfrac{[H^+]}{K_2} + 2\right)} \tag{3.42}$$

Using equation (3.36), $[OH^-]$ can be replaced by $K_w/[H^+]$ in equation (3.42). Consequently, the total carbonic species concentration, TIC in equation (3.14), can be described as:

$$TIC = \left(1 + \frac{K_2}{[H^+]} + \frac{[H^+]}{K_1}\right)\left(\frac{[NH_4^+] + inert - \dfrac{K_w}{[H^+]} + [H^+]}{1 + 2K_2/[H^+]}\right) \tag{3.43}$$

Finally, using equation (3.43), $[H^+]$ and then $pH = -\log_{10}[H^+]$ can be calculated for known TIC and N_T concentrations (both of them (mol/m³) here) obtained from the mass balance equations. Following this further, the dissolved carbon dioxide concentration which is one of the key components can be calculated using equation (3.41).

3.2 CO_2 Supply

In the case of supplying CO_2 into the system, it is supposed that gas is injected at the bottom of the pond through a number of orifices. The aforementioned f_{CO_2} which is the rate of CO_2 supply per unit pond volume, is expressed according to the following equation (Yang, 2011):

$$f_{CO_2} = \frac{1}{Z} \int_0^Z (k_{lb}.a)(CO_{2B}^* - CO_{2D})dz \tag{3.44}$$

Under the assumption that dissolved CO_2 variation along the pond height is negligible, f_{CO_2} will be:

$$f_{CO_2} = (k_{lB}.a)(CO_{2B}^* - CO_{2D}) \tag{3.45}$$

where k_{lB} is the CO_2 mass transfer coefficient from the bubbles to the liquid phase (m/hr), a is the interfacial area between the bubbles and liquid phase per unit volume (1/m), and CO_{2B}^* is the saturation concentration of the dissolved CO_2 (g/m³) in equilibrium with the CO_2 in the bubbles, obtained from Henry's law.

$$CO_{2B}^* = H_{CO_2}P_{CO_{2B}} \tag{3.46}$$

$P_{CO_{2B}}$ is the CO_2 partial pressure in the supply flow (atm) and equals $P_{CO_{2B}} = x_{CO_{2B}}P$, where $x_{CO_{2B}}$ and P are the CO_2 molar fraction and the total pressure of supplied gas (atm), respectively.

Assuming all bubbles are spherical with the same size, the specific mass transfer area of one bubble is (Yang, 2011):

$$a_B = \frac{\pi d_B^2}{\frac{1}{6}\pi d_B^3} = \frac{6}{d_B} \tag{3.47}$$

d_B is the bubble diameter (m). Thus, the interfacial area per unit volume is expressed as (Bhavaraju et al., 1978):

$$a = \frac{6\varepsilon}{d_B} \tag{3.48}$$

ε is the gas holdup and will be discussed later. For calculating d_B, we figured out the previous method used in the literature for the same system (Bello et al., 2017; Yang, 2011) does not fit to the operating condition of the pond and needs to be modified. The procedure proposed by Bhavaraju et al. (1978) is adopted in this work. Indeed, for very low gas rates, bubbles keep constant volume with a size dependent on orifice diameter, surface tension, and buoyancy. A balance between the buoyancy and surface tension forces results in the following equation for d_B:

$$d_B = \left[\frac{6\sigma d_o}{g(\rho_L - \rho_G)}\right]^{1/3} \tag{3.49}$$

where σ is the interfacial tension of CO_2/H_2O (N/m), d_o is the orifice diameter (m), ρ_L and ρ_G are the respective liquid and gas densities (kg/m³), and g is gravity. Equation (3.49) is valid for gas flow rates per orifice (Q_o, m³/hr) smaller than transition gas rates (Q_T, m³/hr) calculated from the following relations:

$$Q_o \leq Q_T = \frac{\pi g(\rho_L - \rho_G)}{108\mu_L}\left[\frac{6\sigma d_o}{g(\rho_L - \rho_G)}\right]^{4/3} \qquad for\ Re_B < 1 \tag{3.50}$$

$$Q_o \leq Q_T = 0.38g^{1/2}\left[\frac{6\sigma d_o}{g(\rho_L - \rho_G)}\right]^{5/6} \qquad for\ Re_B \gg 1 \tag{3.51}$$

Re_B is the bubble Reynolds number:

$$Re_B = \frac{\rho_L u_B d_B}{\mu_L} \tag{3.52}$$

μ_L is the liquid viscosity (Pa.s), and u_B is the bubble rise velocity (m/s) and can be estimated by

Stokes' relation:

$$u_B = \left(\frac{g\rho_L}{18\,\mu_L}\right) d_B{}^2 \qquad for\ Re_B < 1 \tag{3.53}$$

Now that Re_B can be calculated, Q_T is computed from equation (3.50) if $Re_B < 1$ and if $Re_B \gg 1$,

equation (3.51) is used to calculate Q_T. It must be noted that if $Re_B \gg 1$ using the velocity

calculated from equation (3.53), u_B needs to be modified using Mendelson's relation (Bhavaraju

et al., 1978):

$$u_B = \left[\frac{2\sigma}{\rho_L d_B} + \frac{g d_B}{2}\right]^{0.5} \qquad for\ Re_B \gg 1 \tag{3.54}$$

After estimating u_B, k_{lB} can be approximated from the relation (Bhavaraju et al., 1978):

$$k_{lB} = \left[\frac{4D_{CO_2} u_B}{\pi d_B}\right]^{1/2} \tag{3.55}$$

For moderately high gas rates above the Q_T values obtained from equations (3.50) and (3.51), d_B

is computed from a different correlation (Bhavaraju et al., 1978). Since Q_o for this work stays well

below Q_T, those relations for d_B are not discussed here.

Q_o, the gas volumetric flow rate per orifice is obtained by:

$$Q_o = \frac{Q}{nA} \tag{3.56}$$

Q is the total gas volumetric flow rate (m³/hr), n is the number of orifices per unit area (1/m²), and A is the total pond surface area (m²).

To determine the gas holdup which indicates the gas volume fraction in the liquid, the following equation can be used (Shang et al., 2010; Yang, 2011):

$$\varepsilon = \frac{nf\pi d_B^3}{6u_{gB}} \tag{3.57}$$

where f is the frequency of bubble formation at each orifice (1/s) and u_{gB} is the bubble ascending velocity (m/s). f can be obtained by dividing Q_o by the volume of each bubble (Shang et al., 2010):

$$f = \frac{6Q_o}{\pi d_B^3} \tag{3.58}$$

The bubble ascent velocity, u_{gB} can be approximated using a force balance exerted on a detached bubble in its surrounding liquid. With the assumption that inertial forces are negligible, buoyancy (F_b) and drag (F_d) forces will be dominant (Shang et al., 2010). According to Zhang and Shoji (2001), these forces are determined as:

$$F_b = \frac{\pi d_B^3}{6}(\rho_L - \rho_G)g \tag{3.59}$$

$$F_d = \frac{1}{8}\rho_L \pi d_B^2 C_D u_{gB}^2 \tag{3.60}$$

C_D is the drag force coefficient and equals (Zhang and Shoji, 2001):

$$C_D = \frac{18.5}{Re_B^{0.6}} \qquad for\ 1 < Re_B < 1000 \tag{3.61}$$

$$C_D = 0.44 \qquad for\ Re_B > 1000 \tag{3.62}$$

By neglecting gas density since $\rho_G \ll \rho_L$, the force balance, $F_b = F_d$ results in (Shang et al., 2010):

$$u_{gB} = \sqrt{\frac{4gd_B}{3C_D}} \tag{3.63}$$

Using this, the gas holdup is calculated from equation (3.57).

To sum up, the proposed mathematical model describes the behavior of the algal-bacterial consortium in a wastewater pond with the potential to produce lipid for biofuel production. The developed model in this work accounts for the pH estimation with a simpler method while including the effect of nitrogen. Another approach is employed here for calculating the CO_2 mass transfer coefficient when it is sparged into the pond since we realized the method used in the literature (Yang, 2011) for the same system does not fit in the operating condition. Moreover, the Reynolds number in estimating the gas holdup stated in ref. (Yang, 2011) was modified. The other feature of the model as mentioned above is the incorporation of the lipid formation equation with the dynamic prediction of its coefficients, making its model flexible according to the process condition. The system of differential equations is capable of describing the dynamic behavior of the main components in a wastewater treatment process. The simulation method is discussed in the following section.

3.3 Simulation of Dynamic Model

The whole set of equations discussed in the previous section was implemented in MATLAB R2018a. The system of ordinary differential equations (ODEs) was solved using "*ode15s*" function

which is developed for stiff differential equations. It provided the fastest solution amongst the other built-in ODE functions in MATLAB. To determine the dynamic pH values according to the total carbon and nitrogen concentrations in the pond, "*fzero*" function was incorporated in the main ODE function to find the corresponding $[H^+]$ amounts.

3.4 Optimization

Two types of optimization problems were considered in this work. First, for validating the model using experimental data, a parameter estimation problem was solved. We defined the sum of squared errors (SSE) between the predicted values by the model, y_j and experimental data, $\widehat{y}_j$ at specific time points:

$$SSE = \sum_j \left(y_j - \widehat{y}_j\right)^2 \tag{3.64}$$

To estimate the values of model parameters, an optimization method was employed to minimize the SSE, reducing the difference between y_j and $\widehat{y}_j$ values. The selected parameters as decision variables were opted based on their impact on the model prediction using trial and error. Two parameter estimation problems for two different systems were solved in this work. For the first system, the decision variables were: "$inert, K_{l,O_2}, \mu_{Bmax}, Y_{AC}, Y_{BC}, and\ I_s$" and in the second one, the following parameters were chosen: "$K_{l,O_2}, \mu_{Amax}, Y_B, I_s, and\ N_{T0}$".

The second optimization problem was to maximize the lipid production in the continuous wastewater treatment process based on the operating condition. Among the inlet concentrations, nitrogen was dominant in boosting the algal growth and the lipid accumulation, hence it was selected as the decision variable (N_{Tin}). In another case, the amount of bacteria were added to the decision variables as well (X_B). The enhanced algal growth resulted in increased lipid production

and nutrient removal and thus only the lipid formation was set to be maximized by the optimization method.

Among a wide variety of evolutionary algorithms for optimization problems, the particle swarm optimization (PSO) has stood as a significant evolutionary global optimization algorithm (Chu et al., 2011). The major strength of this algorithm is its fast rate of convergence compared to other global optimization algorithms like genetic algorithms (GA) (Abraham et al., 2006). This algorithm uses the interaction of individuals in a population of particles to search complex spaces to find their optimal regions (Clerc and Kennedy, 2002). Thus, PSO was applied in our work to minimize the objective function, f (Kasiri et al., 2015; Zhang et al., 2004):

$$\min_{x} f(x)$$

$$x \in S \subset \mathbb{R}^n \tag{3.65}$$

In the first optimization problem, the objective function was:

$$f = SSE \tag{3.66}$$

And in the second problem, it was:

$$f = -P(t) \tag{3.67}$$

The algorithm initializes with a swarm of particles having random positions x_i (i is the current iteration's index) and velocities v_i to assess the objective function f according to particles positional coordinates. At each time step, positions and velocities are updated, hence f is determined with new coordinates (Clerc and Kennedy, 2002). Each particle stores its own best-ever position in a vector $\hat{x}_i$. The velocity vector v_i updates the position of each particle using the following relations (Abraham et al., 2006; Chu et al., 2011):

$$v_i = wv_{i-1} + c_1 r_1(\hat{x}_i - x_{i-1}) + c_2 r_2(\hat{g} - x_{i-1}) \tag{3.68}$$

$$x_i = x_{i-1} + v_i \tag{3.69}$$

where v_{i-1} is the particle's velocity in the previous iteration, x_{i-1} is the particle's previous position, $\hat{g}$ represents the swarm's best-ever position, w is called inertia weight, r_1 and r_2 are random values in the interval $[0,1]$ which are used to maintain the diversity of the population, and c_1 and c_2 are positive constant coefficients that control the influence of each of the velocity components. Equation (3.68) describes a particle's decision on its next movement, considering its memory of the best experienced position, and the best position found by its most successful particle in the swarm.

The maximum moving distance that a particle can go during one iteration is limited to the range $[-v_{max}, v_{max}]$ (Abraham et al., 2006). v_{max} is a pre-defined relation by user based on the decision variable(s) logical boundary. Since particles have the tendency to fly out of the upper and lower boundaries, it is important to handle the boundary constraints. Random, reflecting, and absorbing schemes are the most popular and basic bound-handling schemes. The PSO algorithm used in this work, performs the reflection scheme. As a result, the boundary acts as a mirror and reflects the projection of the particle's displacement. In Figure 3-3, if $\tilde{x}_i$ is the out of boundary position, the PSO algorithm projects to its final position x_i. x_{i-1} is the particle's position in the last iteration (Chu et al., 2011).
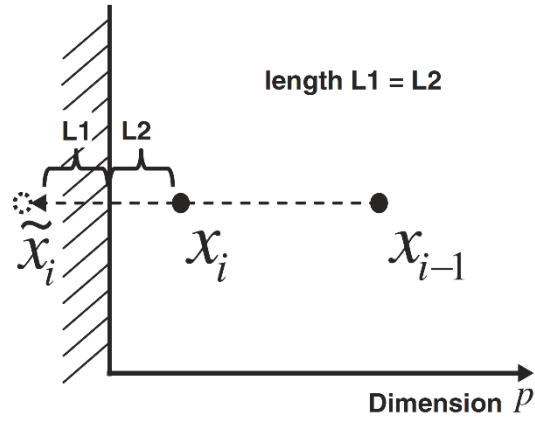
Figure 3-3   Schematic representation of the reflecting scheme (adopted from Chu et al. (2011)*)*

In both problems, the optimization was stopped after some fixed number of iterations without any improvement.

4   Results and Discussion

4.1   Model Validation

The validity of the developed model needs to be verified against experimental data. Table 4-1 defines the values for most of the model parameters introduced in the previous section. Table 4-2 contains the pond specifications and operating parameters considered in the simulation runs. To solve the ode system, reasonable initial concentrations are required. Table 4-3 lists the initial amounts. The parameter values reported in these two tables were utilized in all simulations unless separately represented. There are too few specific experimental results in the literature for wastewater treatment in a high rate algal pond that includes bacteria. The present model is validated using two sets of data for two different systems. The model validation was conducted using the PSO algorithm to minimize the corresponding objective function by finding amounts of some key parameters in each system selected as decision variables. For the first case, the available experimental results in Buhr and Miller (1983) for pH and dissolved oxygen were considered. The data belong to an open algal-bacterial continuous pond and there is no additional CO_2 gas flow into the system. It needs to be noted that the operating temperature (T) was assumed to be constant at 20°C and all the parameters are reported at this temperature unless mentioned.

Table 4-1   Model parameters and their values utilized in the simulations

Parameter	Value	Unit	Reference
Kinetic Parameters			
μ_{Amax}	0.9991	1/days	(Buhr and Miller, 1983; Yang, 2011)
Y_{AO_2}	1.5872	g O_2 produced/	

		g algae produced	
Y_{AN}	0.0913	g N consumed/ g algae produced	
Y_B	2.5	g BOD consumed/ g bacteria produced	
Y_{BO_2}	2.4960	g O_2 consumed/ g bacteria produced	
Y_{BN}	0.1239	g N consumed/ g bacteria produced	
k_{dA}	0.05	1/days	
k_{dB}	0.10	1/days	
K_S	150	g BOD/m³	
K_C	0.044	g CO_{2D}/ m³	
K_{NA}	0.014	g N/m³	
K_{NB}	0.014	g N/m³	
K_{O_2}	0.256	g O_2/ m³	
Physical Properties			
T	20	°C	(Buhr and Miller, 1983; Yang, 2011)
g	9.81	m/s²	
H_{CO_2}	1748.9	g /(m³. atm)	
H_{O_2}	45.2224	g /(m³. atm)	
P_{CO_2}	0.00032	atm	

P_{O_2}	0.21	atm	
D_{CO_2}	1.97e-9 (T=298 K)	m²/s	(Frank et al., 1996)
D_{NH_3}	1.94e-9 (T=293 K)	m²/s	
D_{O_2}	2.1e-9	m²/s	(Akita and Yoshida, 1974)
μ_L	9.07e-4	Pa.s	(Reid et al., 1987)
ρ_L	1000	kg/m³	The approximate value for pure water
$\Delta\rho = \rho_L - \rho_G$	989 (T=298 K, P=0.7 MPa)	kg/m³	(Pereira et al., 2016)
σ	66.95e-3 (T=298 K, P=0.7 MPa)	N/m	
	Equilibrium Constants		
K_W	6.8615e-15	Molar units	(Loewenthal and Marais, 1976)
$pK_1 = -\log_{10} K_1$	6.3819		(Buhr and Miller, 1983; Yang, 2011)
$pK_2 = -\log_{10} K_2$	10.3767		
$pK_A = -\log_{10} K_A$	9.4003		(Bates and Pinching, 1949; Buhr and Miller, 1983)
$pK_B = -\log_{10} K_B$	4.767		(Bates and Pinching, 1949)
	Light Intensity		
K_{e1}	0.32	1/m	(Jupsin et al., 2003)

K_{e2}	0.03	1/m (m³/g)	
I_0	77.8	MJ/(m². day)	(Bello et al., 2017)

Table 4-2   Design and operating parameters

Parameter	Value	Unit	Reference
Pond			
T	20	℃	
Z	0.4	m	(Yang, 2011)
HRT	7	days	(Buhr and Miller, 1983; Yang, 2011)
A	875	m²	This study
Photoperiod (in a 24 h day)	6:00-18:00	h (hour)	(Buhr and Miller, 1983)
Influent Wastewater			
F	50	m³/day	(Yang, 2011)
X_{Ain}	0	g/m³	(Buhr and Miller, 1983)
X_{Bin}	5	g/m³	
S_{in}	590	g/m³	
TIC_{in}	102	g/m³	
N_{Tin}	70	g/m³	
O_{2in}	4	g/m³	
P_{in}	0	g/m³	This study

Supplied CO_2

Q	240	m³/day	(Bello et al., 2017; Yang, 2011)
P	0.11	MPa	(Yang, 2011)
$x_{CO_{2}B}$	0.11		This study
n	250	1/(m²)	(Shang et al., 2010; Yang, 2011)
d_o	0.05	m	(Shang et al., 2010; Yang, 2011)

Table 4-3   Initial concentrations employed in the simulations

Parameter	Value	Unit	Reference
X_{A0}	383	g/m³	(Bello et al., 2017; Yang, 2011)
X_{B0}	5	g/m³	This study
S_0	590	g/m³	
TIC_0	102	g/m³	(Bello et al., 2017)
N_{T0}	70	g/m³	This study
O_{2_0}	4	g/m³	(Bello et al., 2017)

Based on equation (3.23), the initial concentration of lipid in the pond P_0 is obtained as:

$$P_0 = \alpha X_{A0} \tag{4.1}$$

The PSO algorithm gave the best fit between the model prediction and experimental data for the following values of decision variables:

<div align="center">Table 4-4   Estimated parameters for the first model validation</div>

Parameter	Value	Unit
$inert$	1.5019	mol/m³
K_{l,O_2}	0.1000	1/h
μ_{Bmax}	3.7392	1/days
Y_{AC}	2.4663	g CO_2 consumed/ g algae produced
Y_{BC}	2.9411	g CO_2 produced/ g bacteria produced
I_s	16.7856	MJ/(m². day)

Figure 4-1 demonstrates the comparison of oxygen between the model prediction and experimental results available in the literature (Buhr and Miller, 1983). The model follows the experiment's trend; however, there is a discrepancy because the details of feeding pattern were not mentioned and the diurnal light function was different from this work. The coefficient of determination (R^2) for this plot is 0.5561. Figure 4-2 shows that the mathematical model is able to capture a good part of the experimental data for pH. Again, the difference in the light function caused a discrepancy between the observed data and model prediction. The other reason may pertain to the pH estimation method in which we considered the unit activity coefficient for the ions. The R^2 value for this plot is 0.6219. The algae biomass profile in Figure 4-3 (a) follows a similar trend to ref. (Yang, 2011). Algae grow through photosynthesis when the photoperiod starts

by consuming CO_2, hence the plot (b) in Figure 4-3 depicts a decrease in the amount of available carbon dioxide in the pond. At the same time, pH rises because of CO_2 depletion and oxygen amount increases as a result of photosynthesis. The pH values depend on the dissolved CO_2 (acidity) and ammonium ion (alkalinity) concentrations. CO_2 transfers between the pond and atmosphere until its partial pressure reaches equilibrium in the two phases. During this process, a redistribution of the dissolved carbonic species takes place and the concentration of dissolved CO_2 changes. The pH at which the equilibrium is reached depends on the alkalinity of the wastewater in the pond (Loewenthal and Marais, 1976).
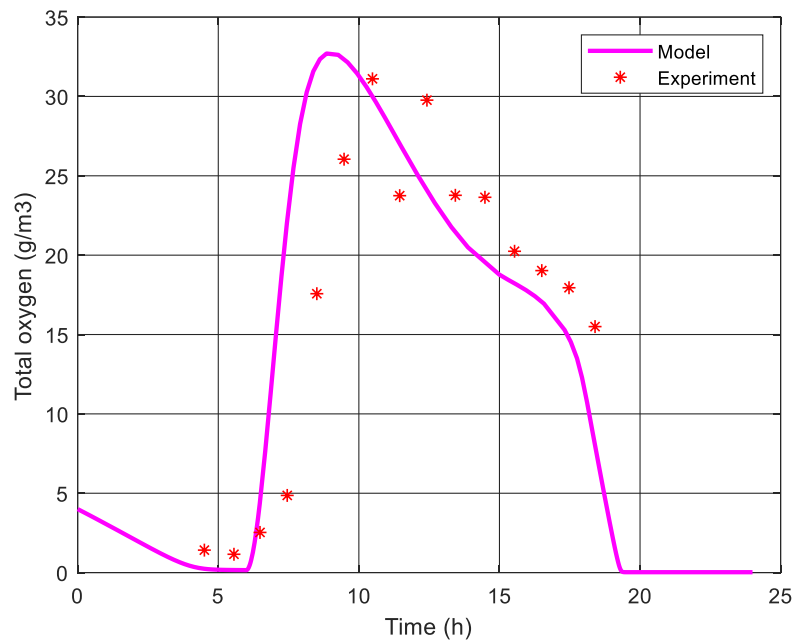
Figure 4-1   Comparison of the model with experimental data
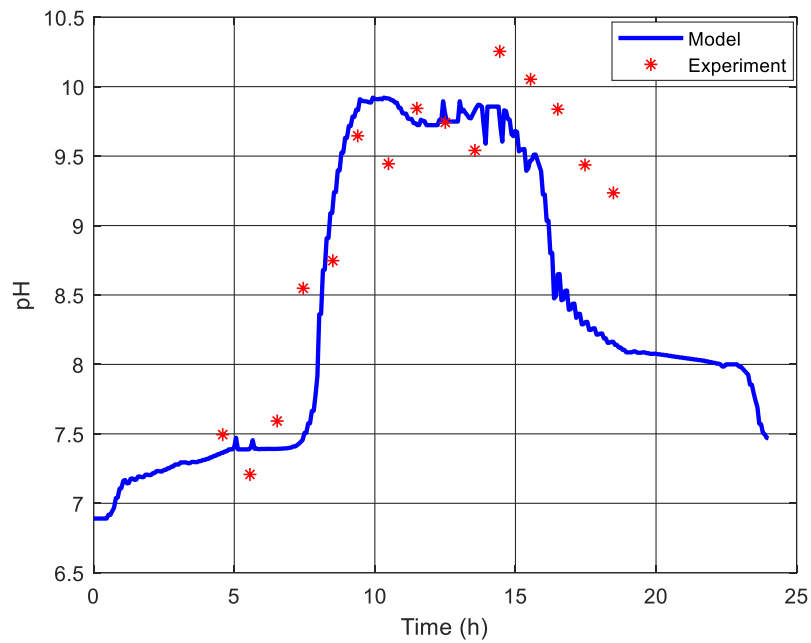
Figure 4-2   pH validation during 24 h period

a   b
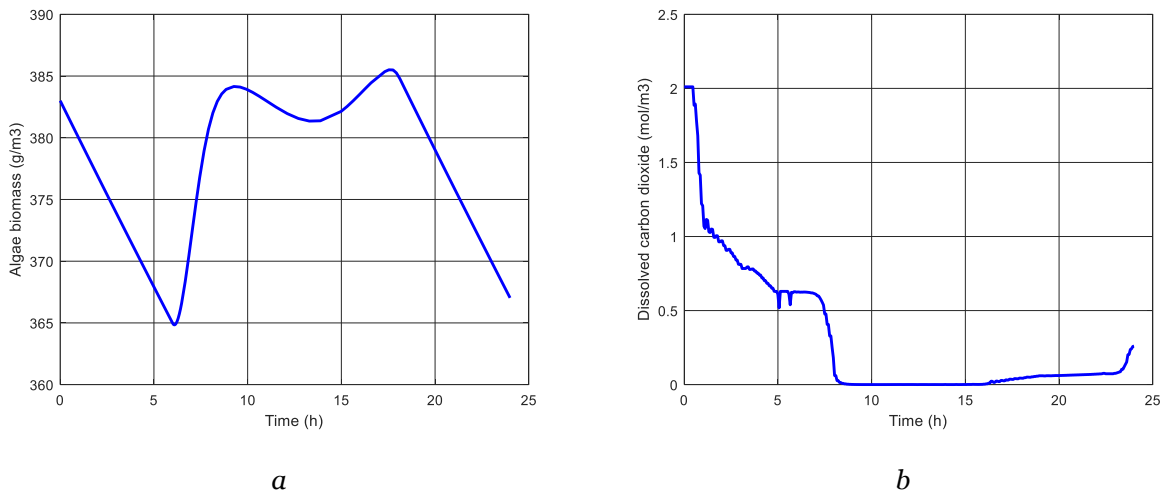
Figure 4-3   Algae biomass and Dissolved CO_2 profiles during 24 h period

The model predictions with a simpler pH estimation method, a different light function, and without having the details of the operating condition were able to provide reasonable results. Moreover, the model was validated against the observed data with tuning of only a few parameters.

The second part of the model validation was completed using the experimental data of Bai et al. (2015) for the algae-bacteria interaction in an open system of a batch process during 7 days. The purpose of their work was to quantify the effect of bacteria on carbon cycling to enhance the algal growth. They also developed a kinetic model to describe the effect of carbon limited algal growth and the role of bacteria in mitigating this effect. Their modeling perspective is different than the current work and only considers the different species of inorganic carbon as nutrient and does not include oxygen and nitrogen. To predict their experimental results using the model developed in this research, the values of some parameters were updated as reported in Table 4-5 and some of them were estimated through the optimization. The remaining ones were kept the same as reported earlier. Note that the estimated concentration for inert ions (*inert*) in the previous part is utilized in all simulations. Since it is a batch process; $F = 0$ and there is no supplied gas; $f_{CO_2} = 0$.

Table 4-5   Updated model parameters values for the second validation

Parameter	Value	Unit	Reference
Kinetic Parameters			
Y_{AC}	2.1829	g CO_2 consumed/ g algae produced	(Buhr and Miller, 1983; Yang, 2011)
Y_{BC}	3.4328	g CO_2 produced/ g bacteria produced	
K_S	0.70	g C/m³	(Bai et al., 2015)
K_C	0.035	g C/m³	
Light Intensity			
I_0	200	$\mu mol\ photons$/(m².s)	(Li et al., 2012)

Initial Concentrations

X_{A0}	90.0	g/m³	(Bai et al., 2015)
X_{B0}	9.10	g/m³	

The PSO algorithm was employed to estimate the values of the following decision variables represented in Table 4-6.

Table 4-6   Estimated parameters for the second model validation

Parameter	Value	Unit
μ_{Amax}	1.0113	1/day
Y_B	0.8834	g BOD consumed/ g bacteria produced
K_{l,O_2}	0.2438	1/h
I_s	67.8416	$\mu mol\ photons$/(m².s)
N_{T0}	121.6922	g/m³

Figure 4-4 shows the comparison between the model prediction and experimental data of the batch process of the algae-bacteria culture. The R^2 value (coefficient of determination) for this plot is 0.9934.
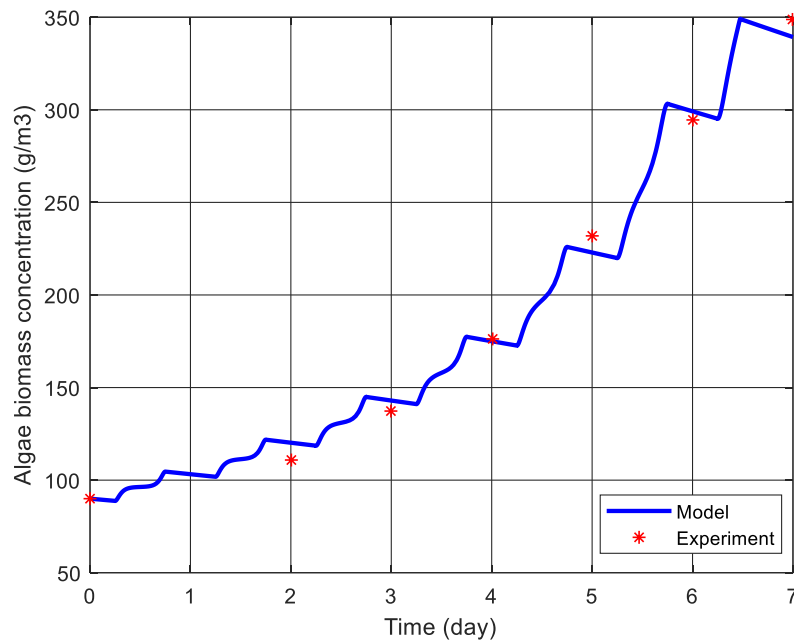
Figure 4-4   Algae biomass comparison plot

4.2 Process Simulation

After developing and validating the mathematical model, the effect of bacteria in enhancing the algal growth was investigated first. Furthermore, we were interested in the predictions of the model for cases when different features such as additional gas supply and a lipid prediction model are incorporated into its main structure. The parameters introduced in Table 4-1 to Table 4-4 were utilized as the base case for all simulation runs unless reported otherwise in the subsequent discussion. From this section onward, the results provided are for the continuous system due to the fact that HRAP systems are inherently continuous raceways (Buhr and Miller, 1983; Craggs et al., 2012).

4.2.1 Pure Algae Pond

To prove that the presence of bacteria promotes the algal productivity, we studied a case with setting the amounts of inlet and initial bacteria and its substrate (BOD) at zero, simulating a pure algal culture. The results are represented in the following plots. Figure 4-5 clearly shows the

advantage of algal-bacterial co-culture due to their mutualistic relationship. The bacteria contribute to carbon cycling and maintain the carbon dioxide for the algae (Bai et al., 2015). The presence of bacteria has promoted the average algae biomass growth by 2.30 %.
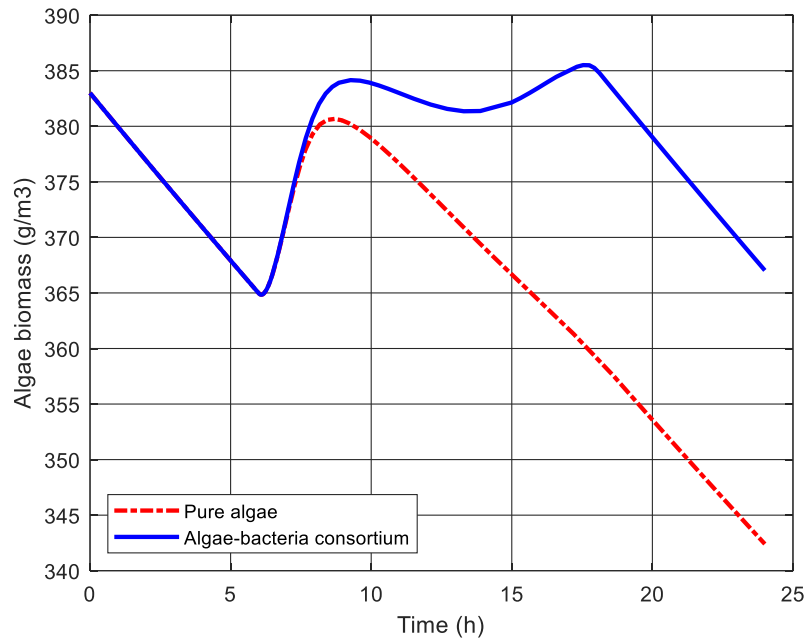
Figure 4-5   Effect of bacteria on the growth of algae

Figure 4-6 compares these two cultures in terms of oxygen (a), dissolved carbon dioxide (b), and pH (c). The oxygen level in the pure culture of algae is higher because there are no bacteria to do respiration and uptake O_2. Additionally, all of the carbon dioxide is consumed by the algae and there is no CO_2 release by the bacteria which can result in carbon limitation in a longer time. However, in the mixed culture of algae and bacteria, CO_2 level is higher compared to the pure culture. The lower level of the dissolved CO_2 in the pure algae pond increases the level of pH. It is been claimed that the algal productivity is higher when pH is low because the amount of available CO_2 for the algae enhances (Bai et al., 2015).
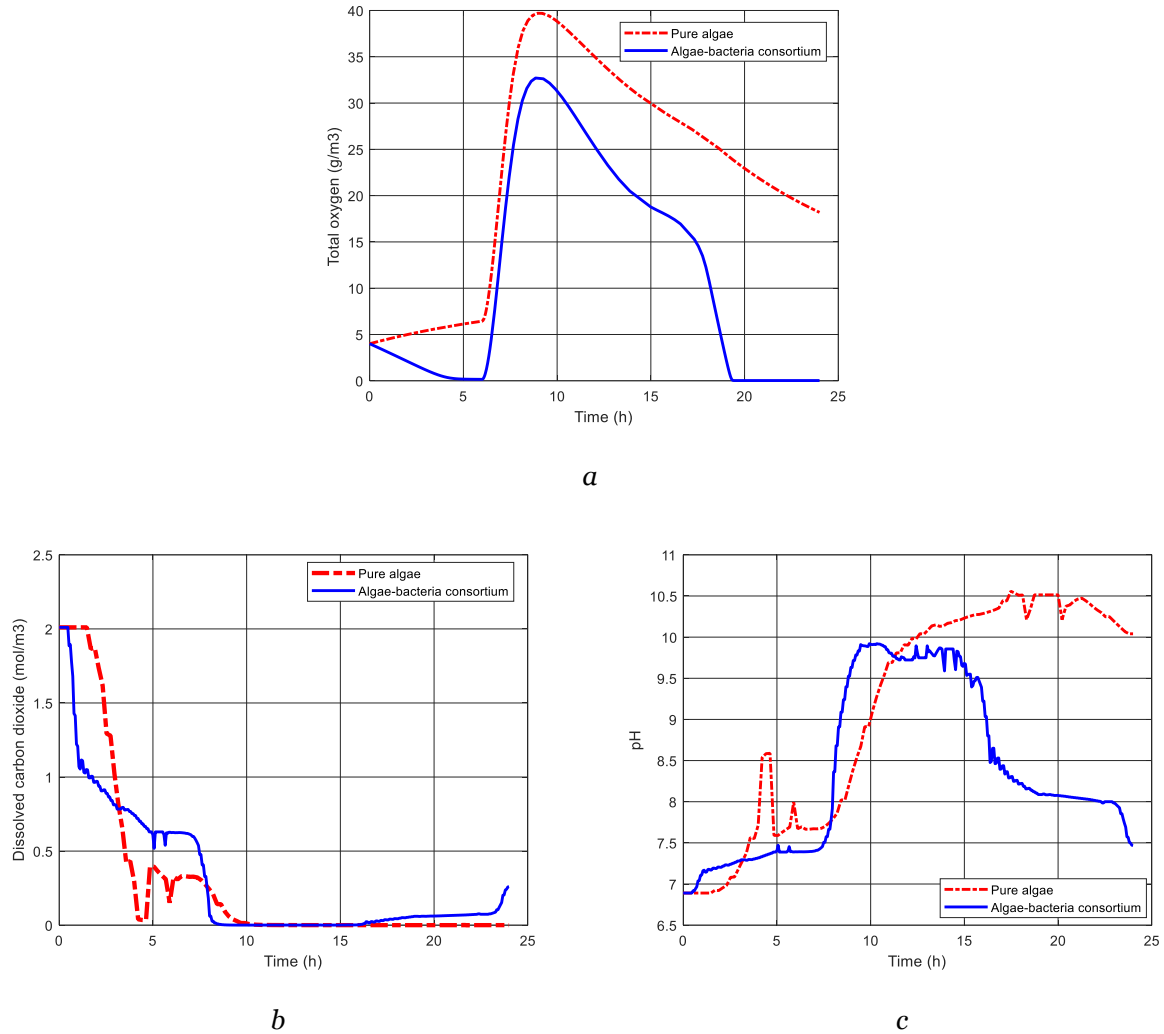
Figure 4-6   Comparison plots between pure algae culture and co-culture of algae-bacteria

4.2.2 CO_2 *Supply*

When the pond is supplied with the additional source of CO_2 being sparged through orifices located at the bottom, more carbon as the substrate is indeed provided for the algae. The contribution toward the algal growth is clearly demonstrated in Figure 4-7. CO_2 supplementation has increased the average amount of algae growth by 8.44% compared to the co-culture of algae and bacteria without providing additional CO_2.
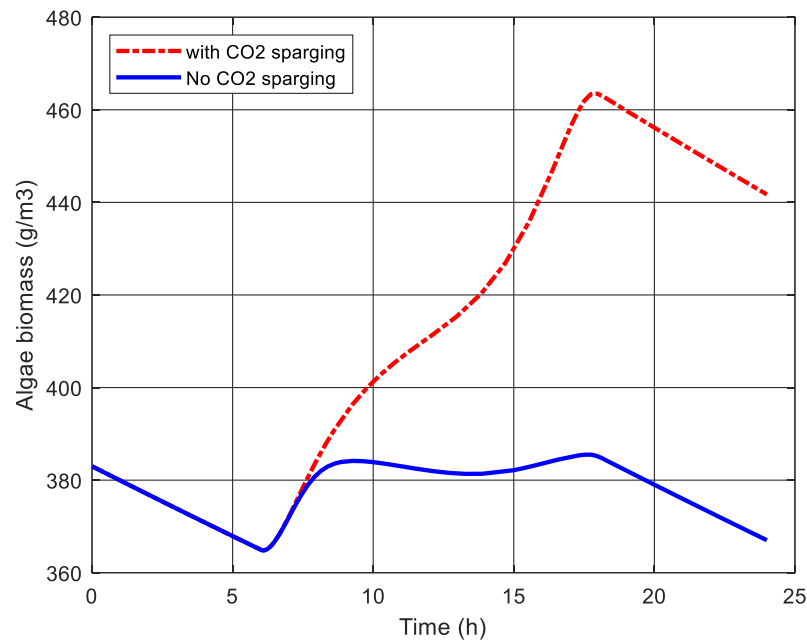
Figure 4-7   Effect of CO_2 supply on the growth of algae

The enhanced level of algal biomass also promotes the bacterial growth (Figure 4-8, plot a) and increases the substrate consumption (Figure 4-8, plot b). CO_2 injection into the pond changes the behavior of other components such as TIC by boosting the total level of carbon, and oxygen by raising its level due to high production by algae (Figure 4-8, plots (c) and (d), respectively). The opposite trend of dissolved carbon dioxide and pH is obvious in Figure 4-8, plots (e) and (f), respectively. The pH level has decreased to about 6.5. For photosynthesis, algae species generally consume free dissolved CO_2 and as pH values drop to 6.5 and smaller amounts, the dominant form of the inorganic carbon becomes dissolved CO_2 rather than the carbonate and bicarbonate species, resulting in enhancement of the algal growth (James et al., 2013).
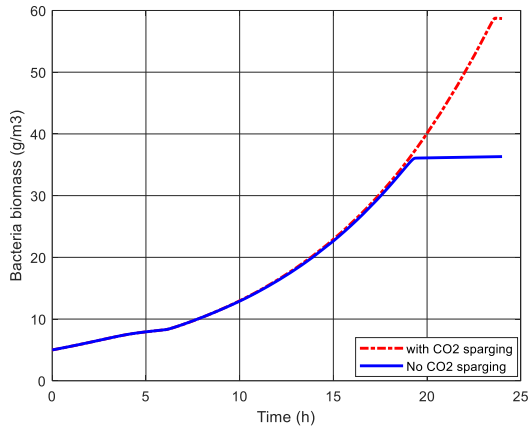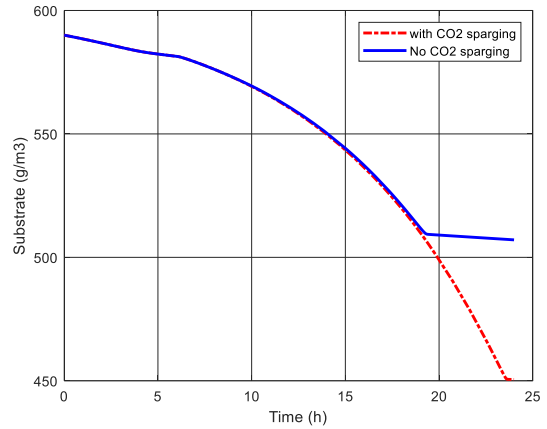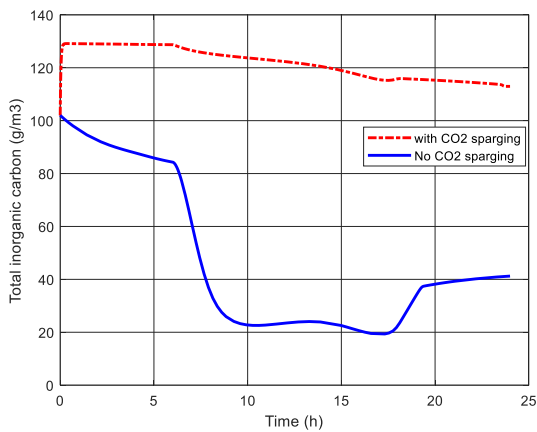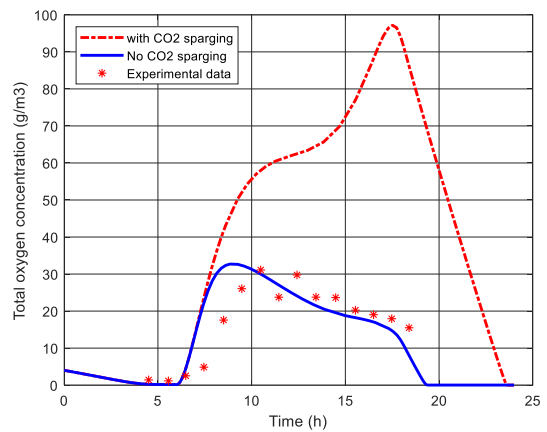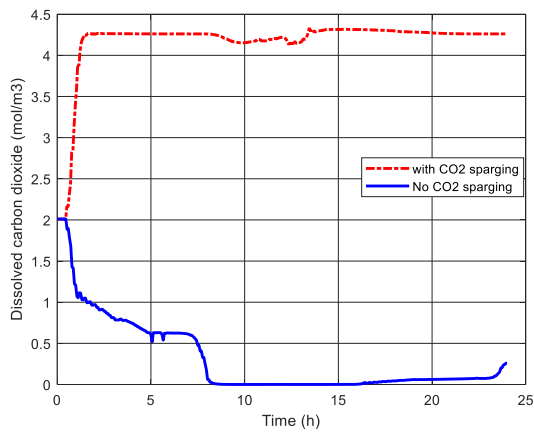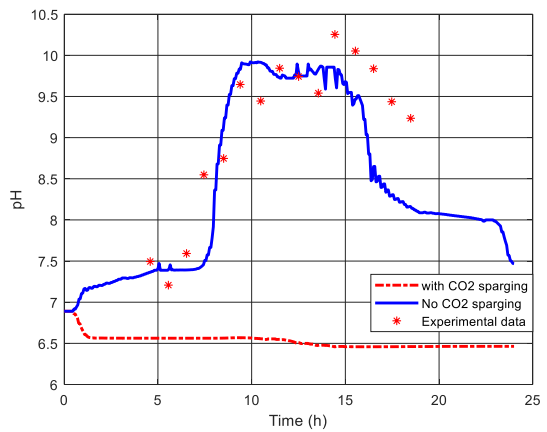
Figure 4-8   Comparison plots showing the effect of CO_2 sparging into the pond

4.2.3 Steady-State Evaluation

The simulations so far were performed during a 24 h period. To simulate a real operating system, it is important to know when the system reaches the (cyclic) steady-state. To evaluate this period, we allowed the simulation to run for a longer time, i.e. many days and calculated the sum of squared errors for each component and pH in the last two days of the run. A 20-days period showed the steady-state and because of the sinusoidal light function, the system reaches cyclic steady-state. The values of SSE are presented in Table 4-7.

Table 4-7   Sum of squared errors for steady-state assessment

Item	Days 18-19	Days 19-20
Algae biomass	0.0663	0.0453
Bacteria biomass	0.0066	0.0039
Substrate (BOD)	0.0011	0.0009
Total inorganic carbon	4.0412e-05	2.5548e-05
Total nitrogen	0.0001	7.1102e-05
Oxygen	0.0055	0.0046
Dissolved CO_2	0.0393	0.0420
pH	0.0062	0.0090

The corresponding profiles at steady-state are shown in Figure 4-9, plots (a-h). It must be noted that the represented graphs below are considered as the "base case" in this work and further evaluations will be compared to this state. The cyclic steady-state profiles demonstrate a better perspective of the concentration and pH changes in the pond. During the first three days, there is a fast increase in the algal and bacterial biomass growth (plots a and b, respectively) and at the same time a sudden decrease in the nutrients consumption including the substrate (plot c), total

inorganic carbon (plot d), and total nitrogen (plot e). The oxygen level in the plot (f) shows fluctuations in days 1-3 that may be due to reaching a balance between fast production by the algae and fast consumption by the bacteria; however, the fluctuations smooth down after the third day. According to the plot (h), the predicted pH values do not drop below 5.9, providing a suitable environment for the growth of algae since most algae species cannot grow well at pH values below 4.5-5.1 (James et al., 2013). The continuous supplementation of CO_2 benefits the mixed culture of algae and bacteria by keeping the pH below 8 (Park and Craggs, 2010).
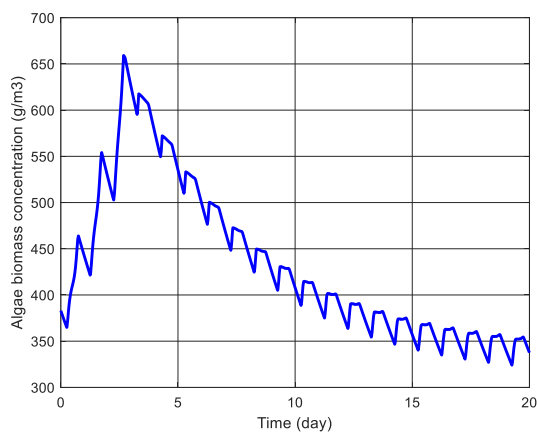
a
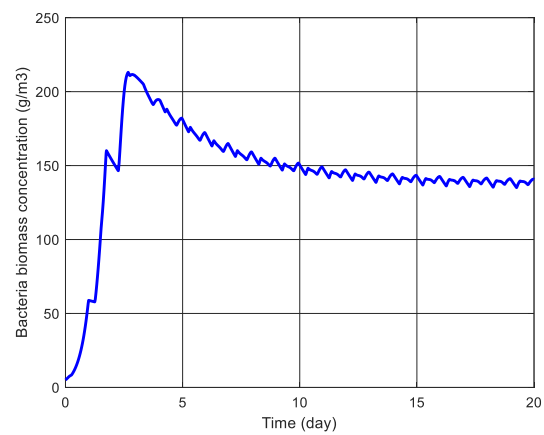
b
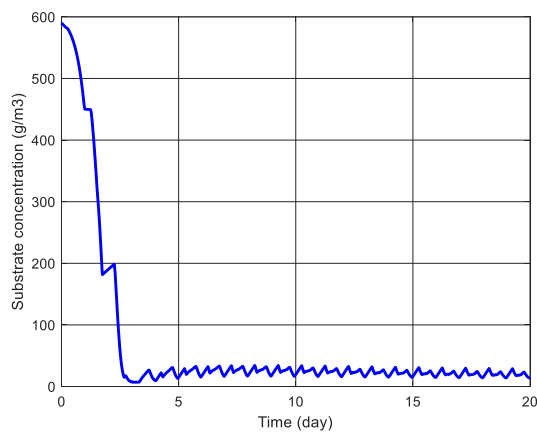
c
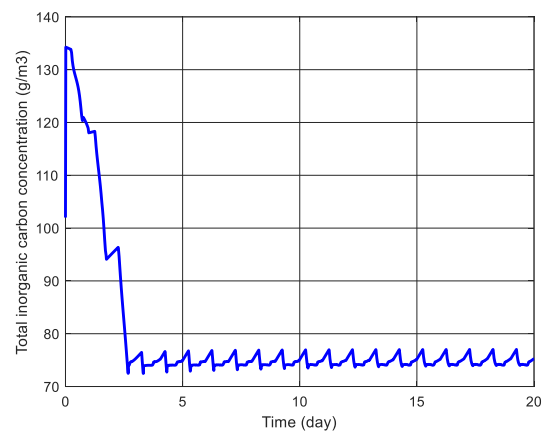
d
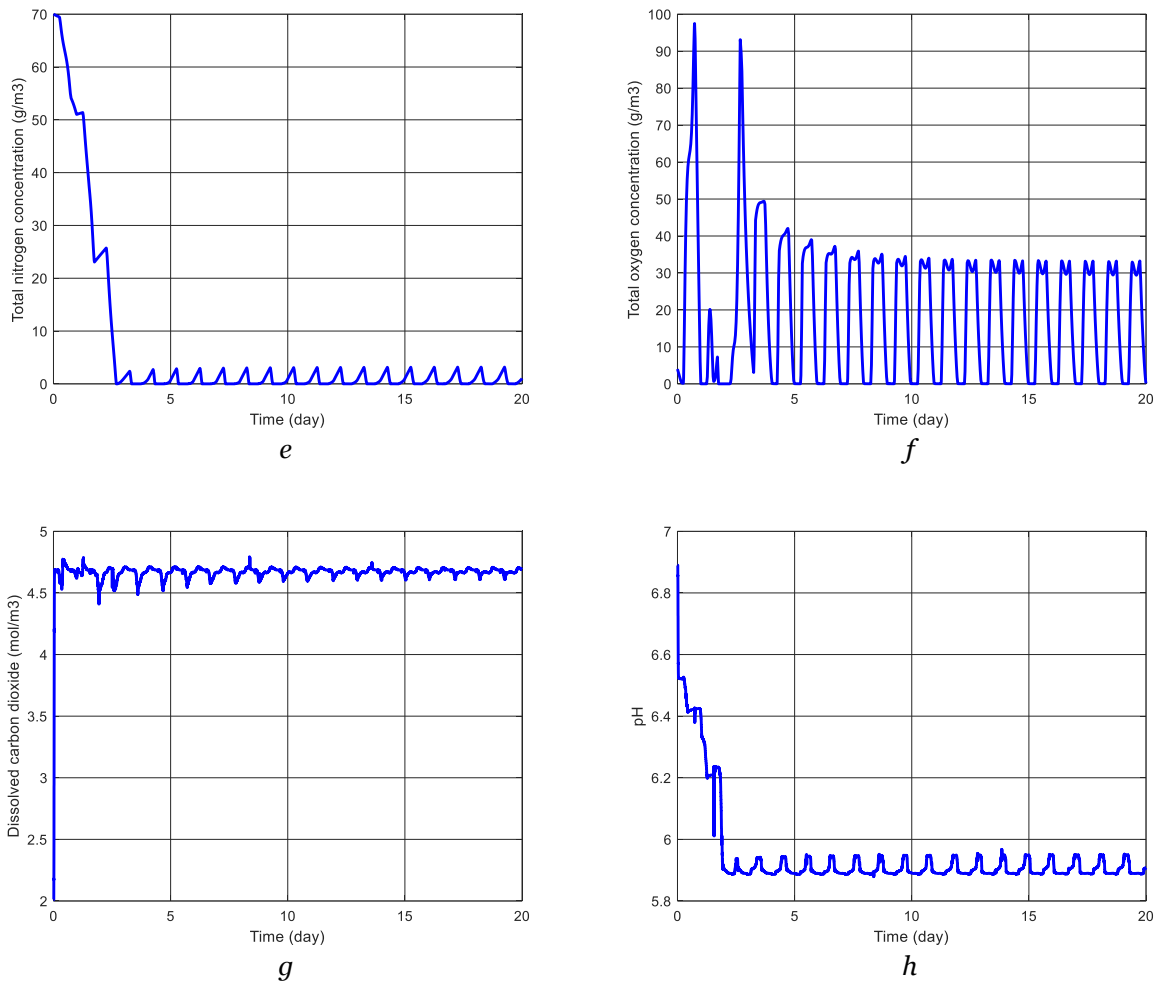
Figure 4-9   Cyclic steady-state plots- Base case

4.2.4 Lipid Production

One of the main goals of this research work was to model lipid production during a wastewater treatment process. The literature studies indicate that algal lipid formation depends on both the cell growth and non-growth coefficients; α and β; equations (3.25) and (3.26), respectively (Deng et al., 2011; Riekhof et al., 2005; Tevatia et al., 2012; Wang et al., 2009). Figure 4-10 demonstrates how the proposed model is able to predict the production of lipids. Although constant α and β were considered in the literature (Surendhiran et al., 2015), (Tevatia et al., 2012; Yang et al., 2011a), it appears to be logical to incorporate dynamic coefficients based on correlations, since the amount of nitrogen and algae biomass are variable; using this resulted in a reasonable lipid

profile. There were no researches available studying the lipid production in a wastewater treatment pond similar to the current work and at the cyclic steady-state system; however, the predicted lipid trend is similar to the profiles published elsewhere for batch cultures at lab scale in a photobioreactor and flask (Surendhiran et al., 2015), (Packer et al., 2011; Tevatia et al., 2012; Yang et al., 2011a).

According to the proposed model, there is an interplay between the amount of algal biomass (Figure 4-11, plot a) and the ammonium ion concentration ($[NH_4^+]$, Figure 4-11, plot b) in the lipid production. As the ammonium ion concentration decreases, lipid accumulation increases. This result has been well established that in nutrient deficiency conditions, microalgae generally accumulate more lipids. Hence, at low or depleted nitrogen concentration, lipid formation enhances (Surendhiran et al., 2015), (Deng et al., 2011; Packer et al., 2011; Tevatia et al., 2012; Work et al., 2010). Indeed, it has been claimed that under the nitrogen-deficient condition, microalgae degrade nitrogen-containing macromolecules and accumulate carbon reserve compounds (particularly lipids) to maintain the cells (Ahlgren and Hyenstrand, 2003; Hoffmann et al., 2010). Comparing lipid synthesis in Figure 4-10 with the ammonium ion consumption in Figure 4-11 (plot b) indicates that as the nitrogen level drops low at about day 3, the lipid accumulation rises in the algae. Based on the equation (3.25), the growth associated coefficient (α) reduces with the decrease in $[NH_4^+]$ amount while due to the equation (3.26), the non-growth associated coefficient (β) increases. This confirms the abovementioned result that as the nitrogen and ammonium ion amounts reach low levels, the synthesis of lipid becomes more non-growth associated and dependent on the amount of algae itself rather than its growth rate. On the other hand, as also shown by Figure 4-11, the growth of algae directly relies on the nitrogen and the reduction in the ammonium level leads to a decrease in the algal growth which affects the lipid production after about day 15.
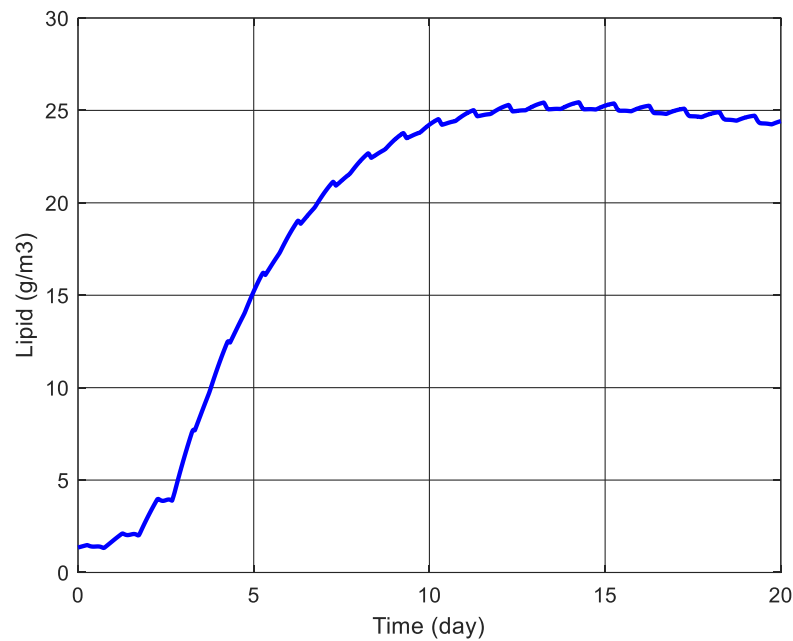
Figure 4-10   Prediction of the lipid production- Base case

a

b
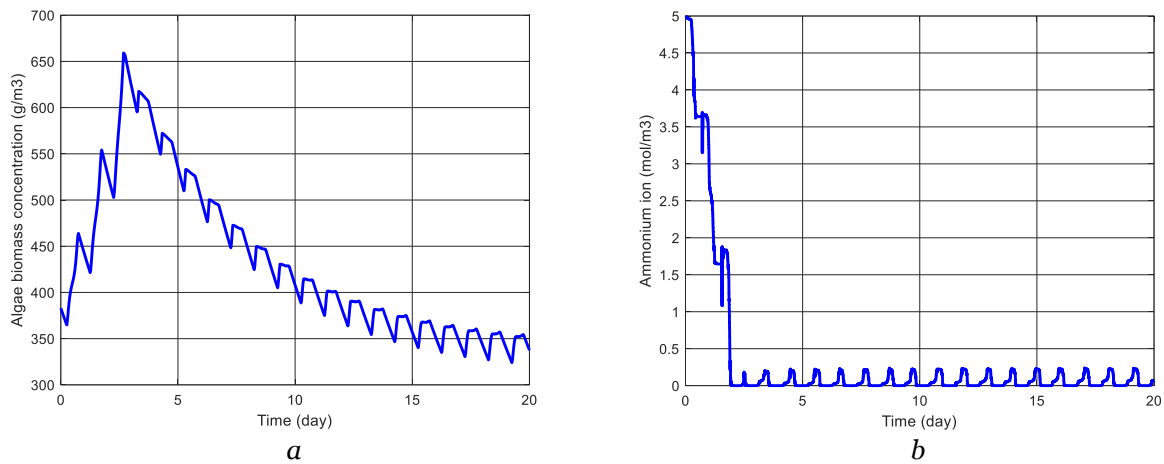
Figure 4-11   Algae growth (plot a) and ammonium ion concentration ($[NH_4^+]$- plot b) profiles

4.3 Process Optimization

After developing a validated model that simulates a wastewater treatment process and predicts production of lipids in a mixed culture of algae-bacteria, we were interested in studying the optimum operating condition of the algal pond in terms of maximum lipid synthesis. Among the nutrients including carbon, nitrogen, and oxygen, nitrogen is the most influential one since the

growth of both algae and bacteria depends on it. Moreover, it affects pH and the amount of dissolved carbon dioxide in the pond. We considered four nitrogen feeding intervals during a day (i.e. the feeding rate could be changed every six hours) and looked for the optimum inlet concentrations. Then, we employed this feeding strategy in four different cases for the system listed in Table 4-8.

Table 4-8   Process optimization cases and the relevant decision variables (marked with ✓)

| | | **Decision Variables** | |
Case	CO_2 supply f_{CO_2}	Inlet nitrogen concentrations	Inlet and initial bacteria concentrations
1	on	✓	Constant
2	on	✓	✓
3	off	✓	Constant
4	off	✓	✓

The first case was the algal-bacterial pond with the additional CO_2 supply. In the second case, we were interested in finding the optimum bacterial concentrations alongside the inlet nitrogen amounts. For the third and fourth cases, we turned off the additional CO_2 gas flowing into the pond and studied the system for the optimum nitrogen and then nitrogen and bacteria concentrations, respectively. The corresponding results are presented in the following sub-sections.

4.3.1 Algae-bacteria culture with CO_2 supply

Keeping the values of parameters the same as reported earlier, the decision variables were the four inlet nitrogen concentrations and the objective function was to maximize the lipid

production. The inlet nitrogen amounts were limited by the maximum concentration of the ammonium ion in the pond, which, according to the literature, is around 120 mg/L (~6.5 mol/m³) (de Godos et al., 2010; Ryu et al., 2017). Furthermore, in terms of the maximum lipid synthesis, it is argued that the algal oil content is highly specific to species and growth conditions and there is no known theoretical maximum cell oil content yet. A maximum average of 50% was considered here (Weyer et al., 2010). In fact, the lipid predicted concentrations were monitored according to this limit. Table 4-9 includes the results obtained using the PSO algorithm.

Table 4-9   Optimum inlet nitrogen feed and average algae and lipid concentrations in the first case

Inlet Nitrogen (g/m³)				Average Concentration (g/m³)	
$N_{T\,in\_1}$ (0-6 h)	$N_{T\,in\_2}$ (6-12 h)	$N_{T\,in\_3}$ (12-18 h)	$N_{T\,in\_4}$ (18-24 h)	*Algal Biomass*	*Lipid*
280.0000	265.6085	280.0000	233.4883	1.4496e+03	41.0836

Figure 4-12 depicts the optimal nitrogen feeding strategy for this case:
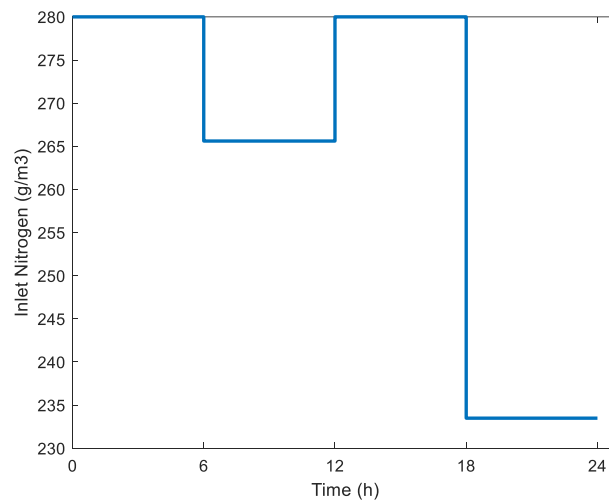
Figure 4-12   Nitrogen feeding pattern in the first case

Figure 4-13 demonstrates the enhanced growth of algae (denoted as "New condition") and compares it with the base case study presented earlier in Figure 4-9 (a). The average concentration of algal biomass is 3.35 times more than the base case.
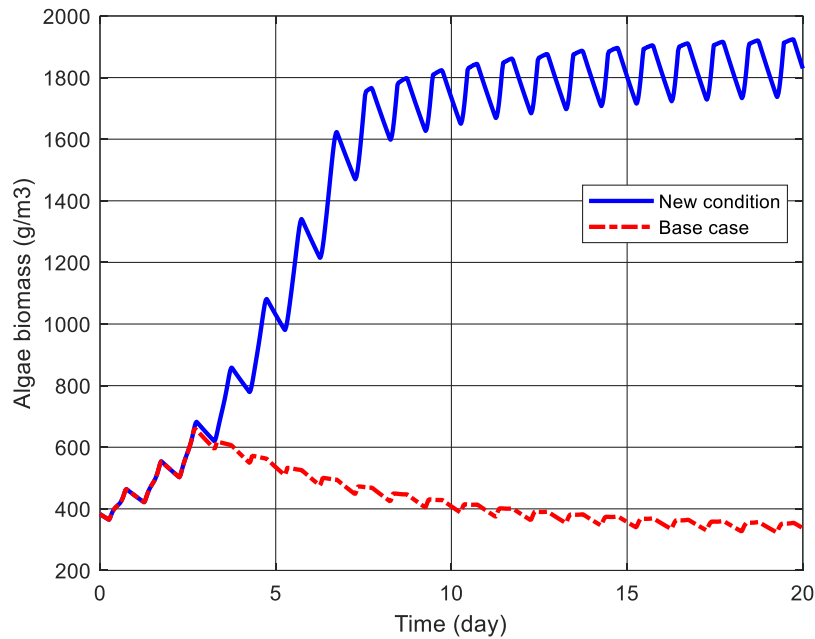
Figure 4-13   Algal biomass growth in the first case

Figure 4-14 shows the increased lipid production when nitrogen is fed at 6-hour intervals in different amounts (denoted as "New condition") and compares it with the base case presented earlier in Figure 4-10. The average accumulated lipid is 2.15 times more than the previous case.
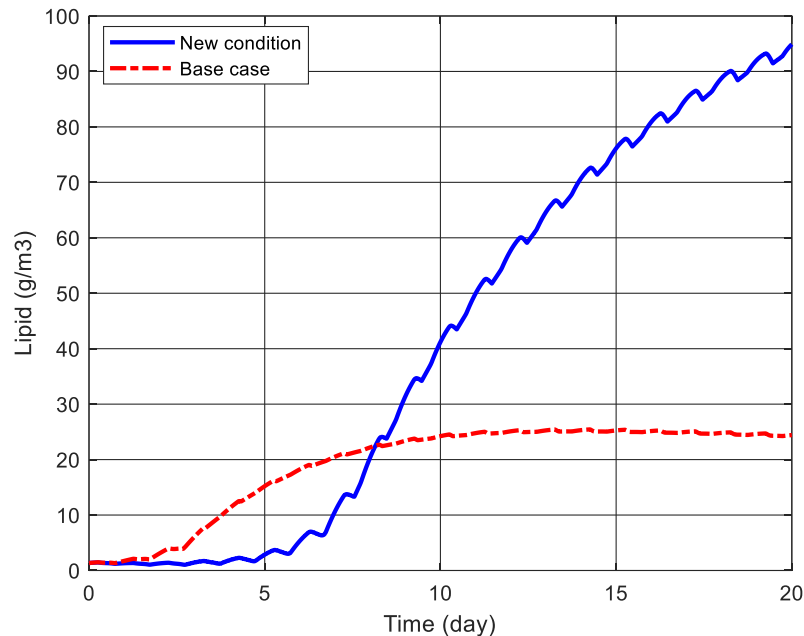
Figure 4-14   Lipid synthesis in the first case

The enhanced amount of nitrogen influences all other components and pH. Figure 4-15 (plots a-h) clearly represents this effect. Nitrogen serves as the nutrient for both the algae and bacteria. The amount of bacterial biomass (plot a) has increased slightly by 1.74% in its average amount which results in more substrate consumption (plot b); there is approximately 14.22% decrease in its average concentration compared to the base case. Plot c shows the increased level of total nitrogen in the pond (the average concentration is about 4 times more than the base condition) that directly boosts the concentration of the ammonium ion (plot g) to nearly 3 times above the average amount of the base case. Due to the increase in algal growth, more CO_2 is consumed by the algae and its average amount is about 3% less than the previous condition (Figure 4-9, plot g). Thus, a rise in pH is anticipated as a result of CO_{2D} decrease and $[NH_4^+]$ increase, which is observed in plot (h). The average amount of pH shows a 1.61% increase. Plot (d) represents the total inorganic carbon concentration, which has increased, and its average is 18.65% more than the average amount in the base case. There are many terms affecting TIC; however, among the amounts of bacteria and algae and CO_2 supply, the overall effect is governed by the increase in the

amount of additional CO_2 supplied into the pond according to equation (3.45). Plot (f) depicts how much more oxygen is produced by the algae (about 9.6 times) and since there is no significant increase in the bacteria growth to perform respiration, the oxygen level is quite high.

a

b

c

d
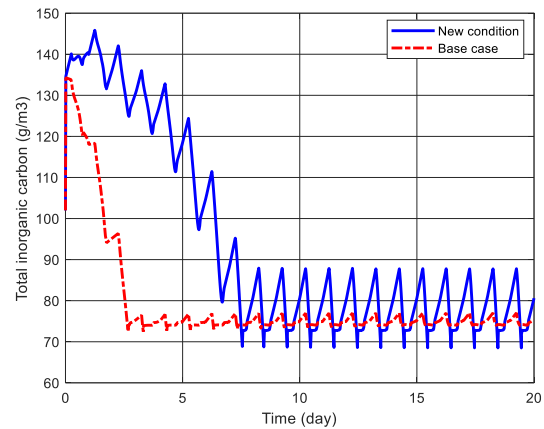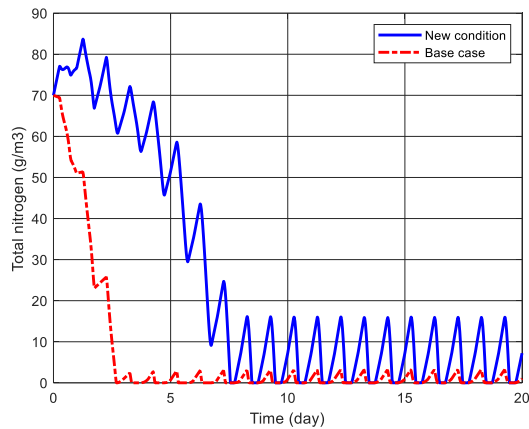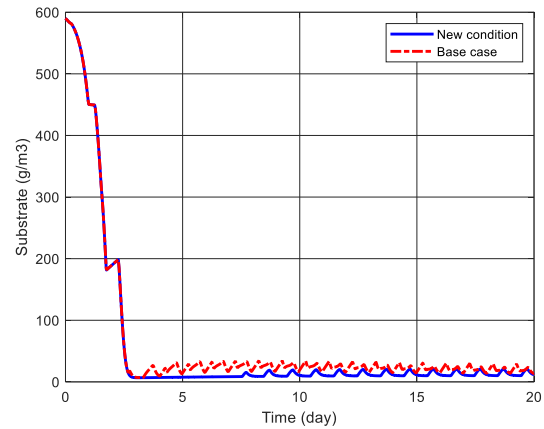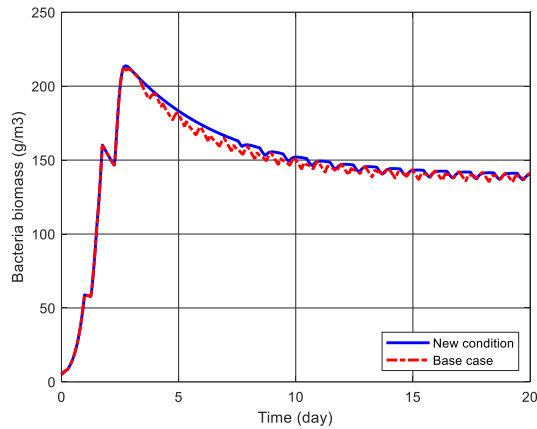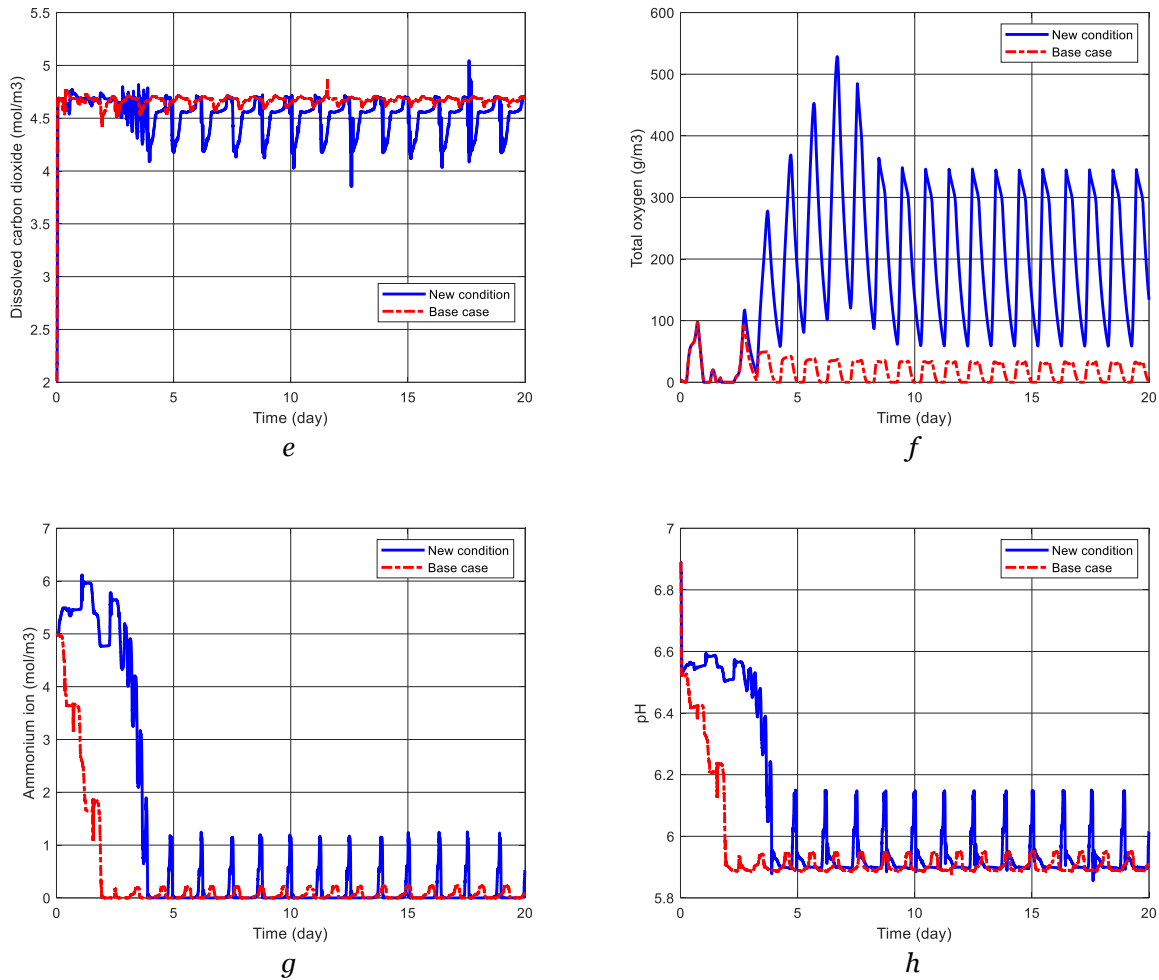
Figure 4-15   Comparison plots between the first case of nitrogen feeding and the base case

4.3.2 Algal culture with CO_2 supply

In this case study, to find the optimum bacteria amounts, we added the bacteria concentration in the inlet flow and the initial condition to be the decision variables in addition to the nitrogen feeding concentrations. Table 4-10 reports the best two results obtained using the PSO algorithm.

Table 4-10 Optimum inlet nitrogen feed, bacteria and average algae and lipid concentrations in the second case

	Inlet Nitrogen (g/m³)				Bacteria (g/m³)		Average Concentration (g/m³)	
	$N_{T\,in\_1}$ (0-6 h)	$N_{T\,in\_2}$ (6-12 h)	$N_{T\,in\_3}$ (12-18 h)	$N_{T\,in\_4}$ (18-24 h)	*Initial* X_{B0}	*Inlet* X_{Bin}	*Algal Biomass*	*Lipid*
I	279.8992	260.304	280.0000	237.2448	2.5790	3.9362	1446.7	40.9082
II	280.0000	278.6921	246.7383	133.5714	2.4961	0.6227	1313.2	40.5610

The suggested nitrogen feeding patterns are represented in Figure 4-16.
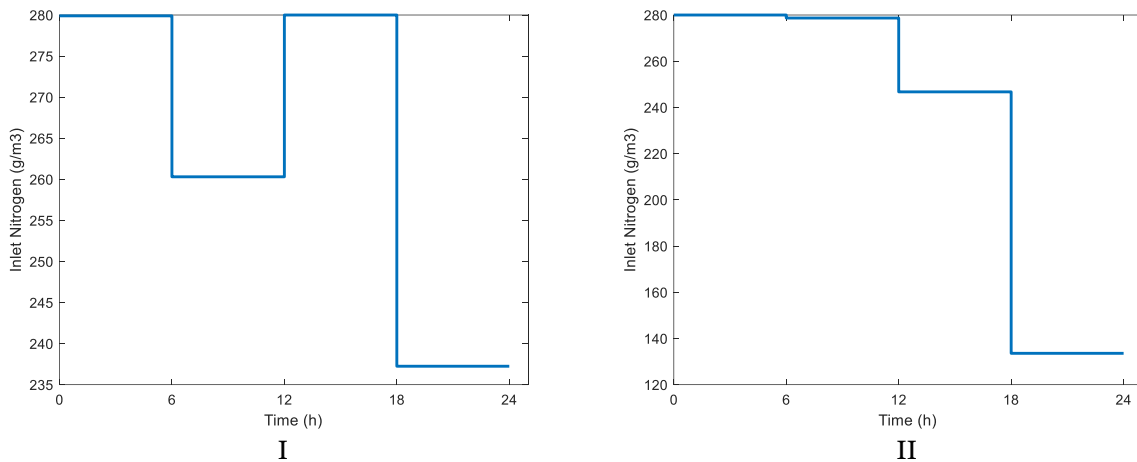
Figure 4-16 Nitrogen feeding patterns in the second case

The predicted optimal condition in **I** is very close to the first case study. However, the predicted state in **II** shows that for lesser amounts of the nitrogen in the feed and bacteria both in the inlet flow and initial condition, the accumulated lipid is almost the same amount as the first case study reported in Table 4-9. However, there is an insignificant decrease in the algal growth of the state

II. The concentration profiles of the components and pH are very similar to the first case study, and thus are not presented in this section. Consequently, the state **II** is capable of producing approximately the same results as the first case study.

4.3.3 Algae-bacteria culture without CO_2 supply

In this case study, we looked for the optimum operating condition when there is no CO_2 supply into the pond, i.e. $f_{CO_2} = 0$. The results found using the PSO algorithm are presented in Table 4-11.

Table 4-11   Optimum inlet nitrogen feed and average algae and lipid concentrations in the third case

	Inlet Nitrogen (g/m³)			Average Concentration (g/m³)	
$N_{T in\_1}$ (0-6 h)	$N_{T in\_2}$ (6-12 h)	$N_{T in\_3}$ (12-18 h)	$N_{T in\_4}$ (18-24 h)	Algal Biomass	Lipid
98.2943	70.0000	70.0000	71.4525	283.6431	13.3045

The optimum nitrogen feeding pattern for the current case is depicted in Figure 4-17.
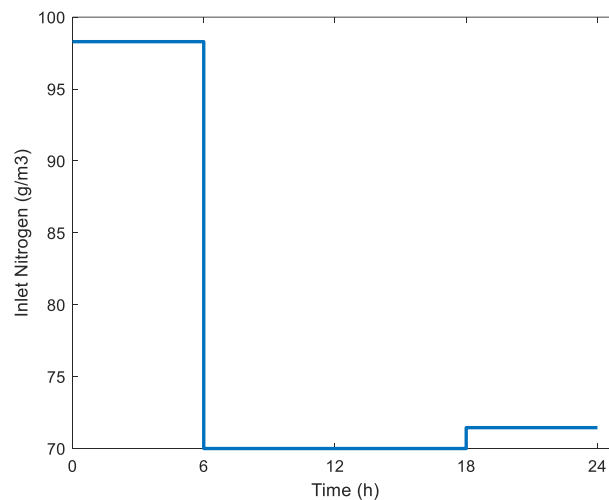
Figure 4-17   Nitrogen feeding pattern in the third case

The predicted optimum inlet nitrogen concentrations are much lower than in the first two case studies. Higher amounts of the nitrogen in the feed results in an increase in the algal growth; however, the lipid synthesis decreases because of the reason mentioned in section 4.2.4.

Figure 4-18 demonstrates the conspicuous effect of turning off CO_2 supply on the algal growth. It shows a 34.5% decrease compared to the base case (Figure 4-9, plot a). The reduction in the amount of the algal biomass affects the lipid accumulation too. As presented in Figure 4-19, the produced lipid is 30.4% less than the base case presented earlier (Figure 4-10).
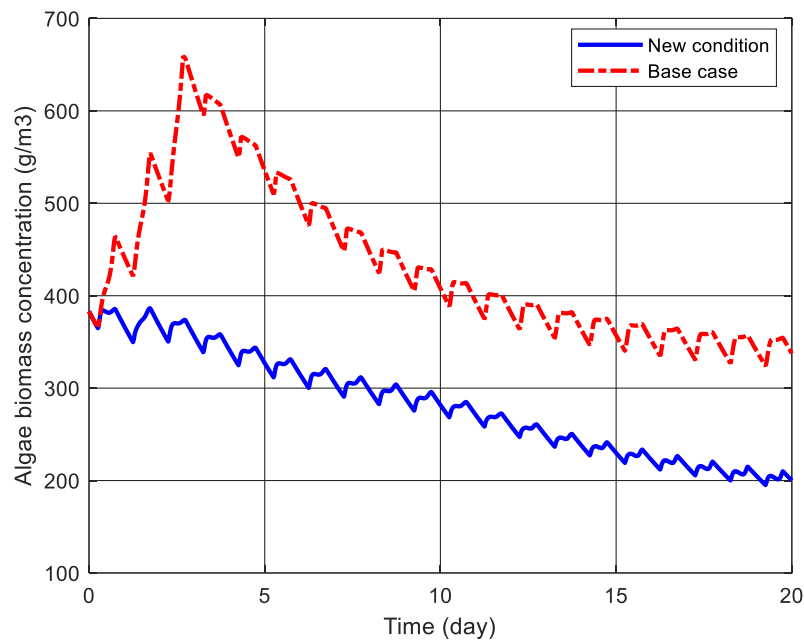
Figure 4-18   Algal biomass growth in the third case
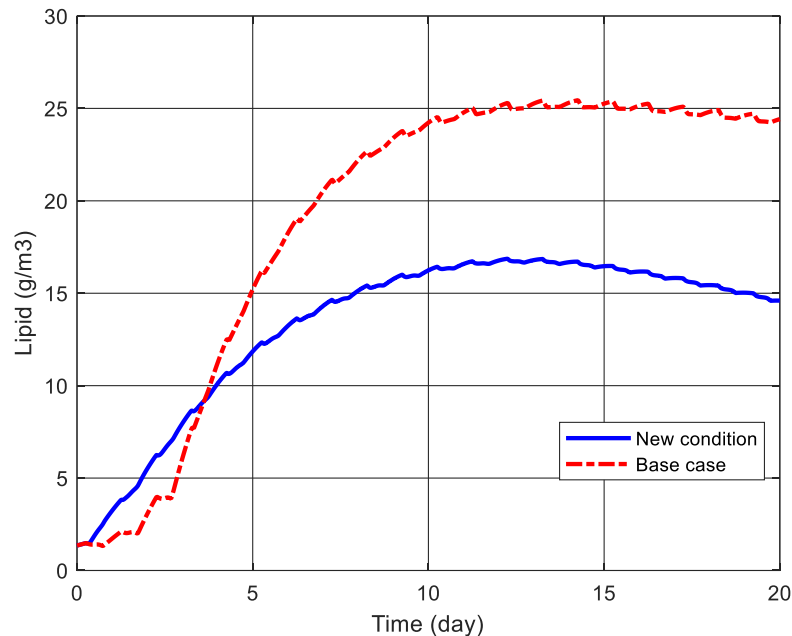
Figure 4-19   Lipid accumulation in the third case

Figure 4-20 shows how turning off CO_2 supply affects the profiles of the other states of the system. Plot (a) demonstrates the decrease in the bacterial growth that is equal to 10.7% in its average concentration for 20 days with the same initial and inlet amounts as the base condition (Figure 4-9, plot b). On the other hand, the substrate consumption decreases (plot b) and there is a 95% increase in its average amount compared to the base case. The increase in the nitrogen concentration due to the enhanced level of the inlet nitrogen is clear in plot (c). The average level has increased by about 26%. Plot (d) shows the decreased amount of the total inorganic carbon in the pond which is equal to 69% in terms of the average concentration. Similarly, the average dissolved carbon dioxide reduces near 98% compared to the base condition. Plot (e) clearly shows this reduction. As expected, pH rises as a result of CO_{2D} decrease and $[NH_4^+]$ increase, which is not appropriate for the algal growth. The average level of pH is enhanced by about 40% (plot h) and the ammonium ion shows almost the same rise (41%) in its average amount (plot g). Due to the reduced level of the algal growth, the oxygen concentration is decreased drastically as shown in plot (f). Its average concentration is 94% less than the base case (Figure 4-9, plot f).

a

b

c

d

e

f

g   *h*
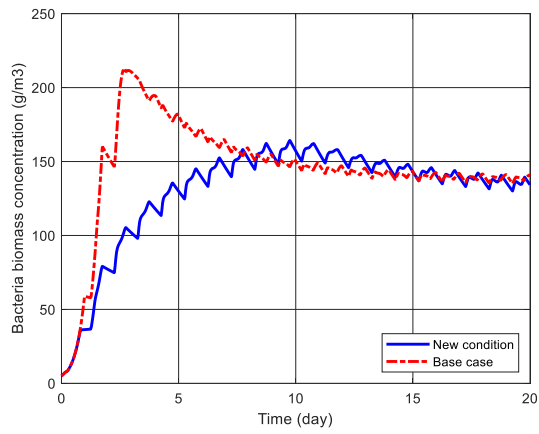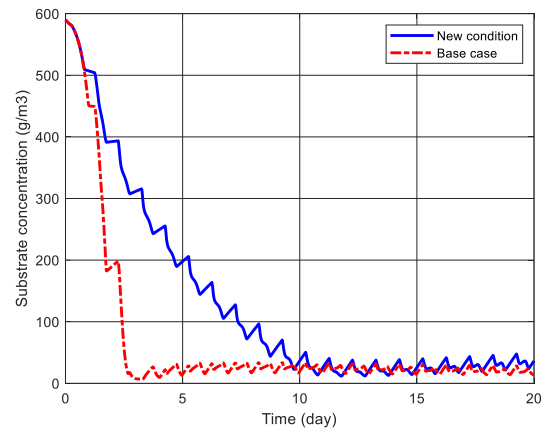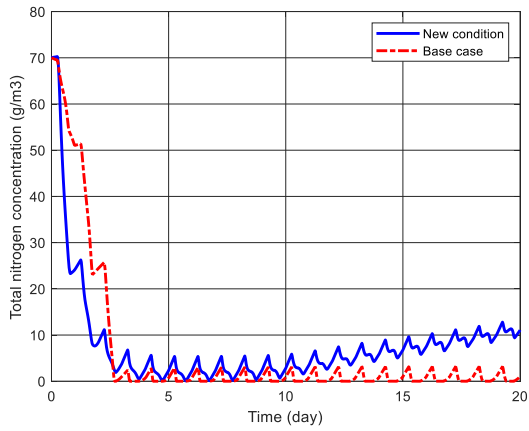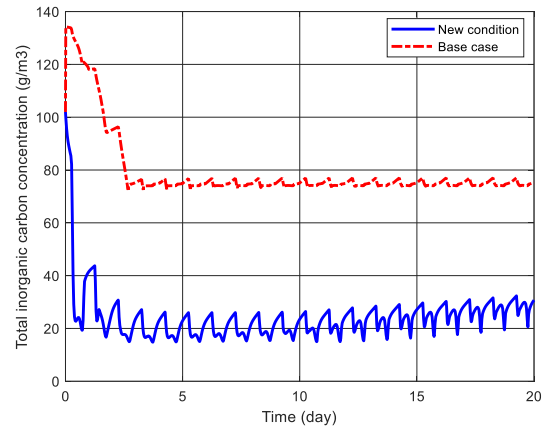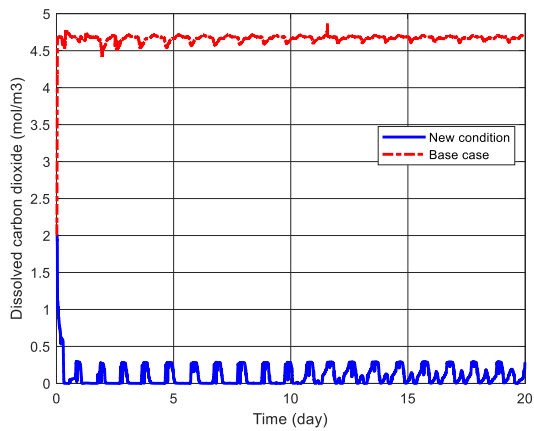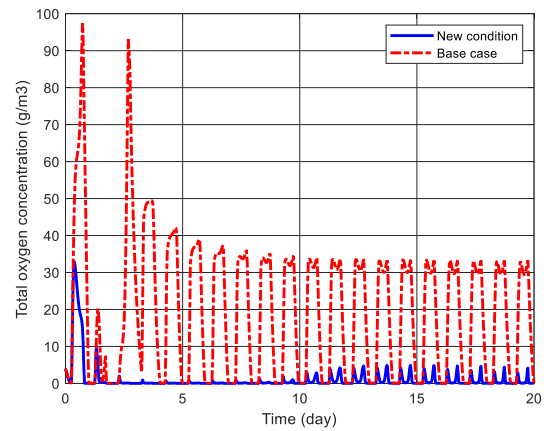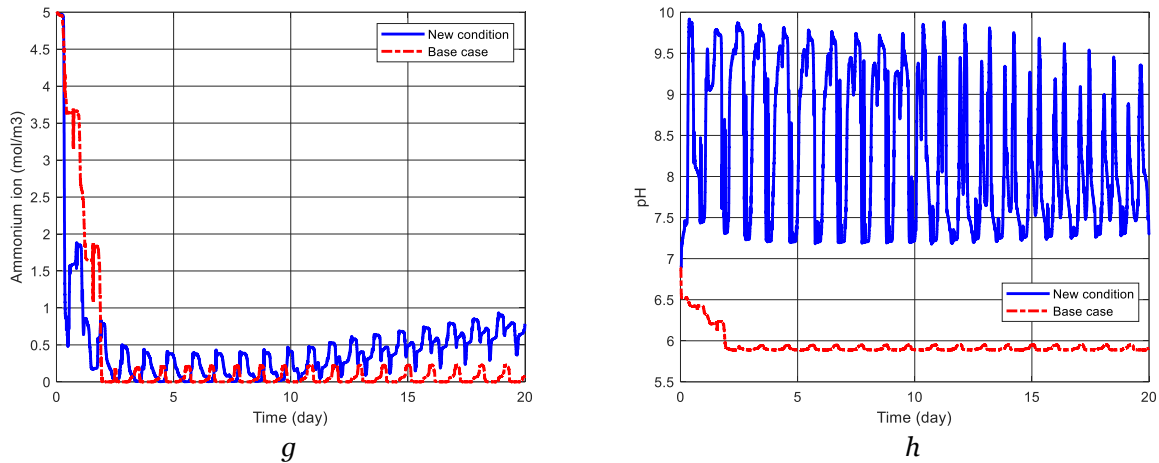
Figure 4-20   Comparison plots between the third case of nitrogen feeding and the base case

4.3.4 Algal culture without CO_2 supply

Similar to section 4.3.2, we chose 6 decision variables including the initial and inlet bacteria concentrations for this case. The best two predicted optimum nitrogen and bacteria concentrations using the PSO algorithm are reported in Table 4-12 and the related feeding patterns are depicted in Figure 4-21. The other profiles look like the ones reported in the previous section (4.3.3); therefore they are not presented in this section.

Table 4-12   Optimum inlet nitrogen feed, bacteria and average algae and lipid concentrations in the fourth case

	Inlet Nitrogen (g/m³)				Bacteria (g/m³)		Average Concentration (g/m³)	
	$N_{T\,in\_1}$ (0-6 h)	$N_{T\,in\_2}$ (6-12 h)	$N_{T\,in\_3}$ (12-18 h)	$N_{T\,in\_4}$ (18-24 h)	*Initial* X_{B0}	*Inlet* X_{Bin}	*Algal Biomass*	*Lipid*
I	70.0000	75.7577	80.1226	70.0000	5.0000	1.0000	281.5584	13.2926
II	82.4064	70.0000	74.1914	70.0000	3.5042	3.8817	280.7061	13.2428

The estimated average lipid concentration in **I** is almost the same as the previous section (4.3.3) and it can be concluded that keeping the initial bacteria concentration at a relatively high level, the inlet bacteria can be fed in lesser amounts. On the other hand, the obtained results in **II** show that for a smaller amount of the bacteria initially available in the pond, if the inlet concentration is increased, the average accumulated lipid is very close to the previously predicted optimum.

The nitrogen feeding pattern helps in promoting the algal growth; however, the absence of the

I   *II*
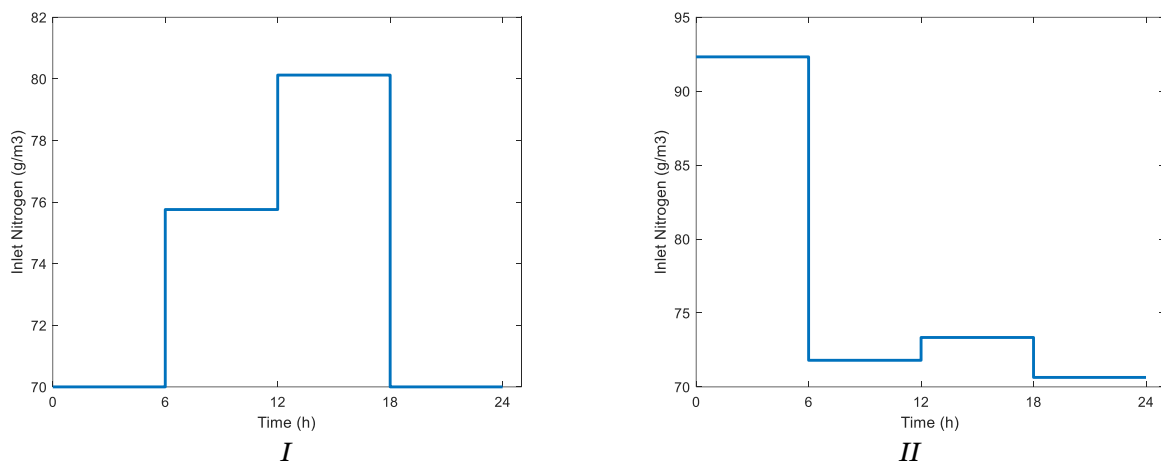
Figure 4-21 Nitrogen feeding patterns in the fourth case

additional source of CO_2 cannot be compensated by altering the amounts of nitrogen and bacteria. Furthermore, there is a limitation on increasing the nitrogen concentration since the algae synthesizes lipid effectively in the nitrogen depleted condition. Increasing the inlet amount of the total inorganic carbon or adding more bacteria in the influent flow is influential in enhancing the algal growth and the lipid production; however, the changes are very small.

To sum up, the process simulation results show that if the mixed culture of algae and bacteria is supplied with the additional source of CO_2 and the nitrogen is concentrated in the influent stream and fed into the pond in a stepwise pattern, the algal growth is boosted dramatically, which results in high lipid production. This fact is confirmed in the literature (Sutherland et al., 2015) that although microalgal wastewater bioremediation HRAPs can potentially provide cost-effective

feedstock for biofuel production, enhancing biomass generation is a high priority to make microalgal biofuel economically viable.

5   Conclusions and Future Work

5.1 Conclusions

Wastewater treatment using microalgae not only contribute to BOD and nutrient removal, but also provide free feedstock for sustainable production of biofuel through biomass generation. The integration of microalgal wastewater bioremediation and bioenergy production in a high rate algal pond is an eco-friendly process and potentially commercially viable if the biomass production is increased. The main purpose of this research was to investigate lipid formation in a wastewater treatment process in an HRAP system through mathematical modeling. Taking advantage of the co-culture of algae and bacteria, the performance of the system was evaluated using process simulation under different operating condition. The important findings of the simulations are as follows:

- The presence of heterotrophic bacteria enhanced the algal growth compared to a pure culture of algae. They improved the carbon cycling by producing CO_2, hence the carbon required for the algal growth is maintained in the pond.

- When the pond is supplied with an additional source of CO_2, i.e. flue gas containing CO_2, two purposes are served: (i) the growth of algae is boosted dramatically, since the dissolved CO_2 is one of the main substrates of the algae, and (ii) it helps in mitigation of the CO_2 footprint in the atmosphere with respect to global warming.

- A lipid production model was successfully incorporated into the structure of wastewater treatment model. The accumulation of lipid required for biofuel generation depends on the algal growth and the concentration of nitrogen in the pond.

- Process simulation results showed that when the pond is subjected to the additional source of CO_2, the increase in the feeding amount of nitrogen further promoted the algal

growth and lipid formation. A stepwise feeding pattern was suggested as the optimum condition.

+ When the CO_2 sparging stream is turned off, the growth of algae reduces significantly followed by a remarkable decrease in lipid accumulation. The increase in the inlet amount of nitrogen improves the algal growth and lipid production; however, it cannot compensate for the absence of CO_2 supplementation. Moreover, the nitrogen feeding concentration cannot reach higher levels since it limits the lipid production in the pond.

+ In general, co-cultivation of algae and bacteria enhances the algal productivity in both CO_2 sparging and not sparging conditions. Nevertheless, if the pond is not supplied with the additional source of CO_2, a higher total amount of bacteria including the inlet and initial concentrations is recommended compared to the CO_2 supplementation condition. In the latter case, lower amounts of bacteria are adequate without making significant changes to the algae and lipid yields.

The obtained results are based on the model developed in this work for describing a generic microalgal-bacterial wastewater treatment process in an HRAP and evaluating the lipid formation for the purpose of biofuel production. The model allows for performing simulation tests under different operational conditions and making predictions about the important characteristics of the system.

5.2 Future Work

+ The model can be extended to make it specific for the type of wastewater and algal and bacterial species to study the lipid production for each system in particular. Various wastewaters have different physical-chemical characteristics (Salama et al., 2017) and the interactions between the algae and bacteria can include all types of symbiotic relationships from mutualism to parasitism. These interactions are strongly dependent on the species

since the microenvironment differs for each algae (Fuentes et al., 2016). Although almost all wastewaters have the major nutrients in common required for the growth of algae, they have different compositions and components including heavy metals that might exert inhibition on the algal growth depending on their concentrations.

- According to the literature (Buhr and Miller, 1983; Jupsin et al., 2003; Yang, 2011) the HRAP can be simulated as a number of serially connected CSTRs to increase the model accuracy in terms of the mixing.

- The biorefinery approach can remarkably improve the biofuel production economics through employing the biorefinery based production strategy. In other words, all the constituents of the biomass raw material can be converted to value-added products such as Docosahexaenoic acid (DHA) and carotenoids in addition to biofuel production. This approach is considered as the best solution to integrate different processes, benefiting the economy and environment and simultaneously reducing waste and pollution (Rawat et al., 2011; Singh and Gu, 2010). Therefore, considering the mixed culture of algae and bacteria to accomplish the ultimate goal of developing a biorefinery can be a novel research work. In this regard, since various process pathways may be involved in designing the biorefinery because of the variety of wastewaters, algal-bacterial species and interactions, developing an optimization model to investigate the optimum process pathway would profoundly help in the process design.

- The work done in this study was mainly a deterministic model solution. Numerous parameters are involved in the algal biofuel production and each of them may differ according to the system and operating condition. It would be time- and cost-effective to recognize the parameters that make uncertainty in the model and develop a stochastic model to consider uncertainties in making the decision for determining the efficient processes.

References

Abraham, A., Guo, H., Liu, H., 2006. Swarm intelligent systems, in: Nedjah, N., Mourelle, L. de M. (Eds.), Studies in Computational Intelligence. Springer. https://doi.org/10.1007/978-3-540-33869-7

Ahlgren, G., Hyenstrand, P., 2003. Nitrogen limitation effects of different nitrogen sources on nutritional quality of two freshwater organisms, *Scenedesmus Quadricauda (Chlorophyceae)* and *Synechococcus sp. (Cyanophyceae)*. J. Phycol. 39, 906–917. https://doi.org/10.1046/j.1529-8817.2003.02026.x

Akita, K, Yoshida, F., 1974. Bubble size, interfacial area, and liquid-phase mass transfer coefficient in bubble columns. Ind. Eng. Chem. Process Des. Dev. 13, 84–91. https://doi.org/10.1021/i260049a016

Azov, Y., Shelef, G., Moraine, R., 1982. Carbon limitation of biomass production in high-rate oxidation ponds. Biotechnol. Bioeng. 24, 579–594. https://doi.org/10.1002/bit.260240305

Bai, X., Lant, P., Pratt, S., 2015. The contribution of bacteria to algal growth by carbon cycling. Biotechnol. Bioeng. 112, 688–695. https://doi.org/10.1002/bit.25475

Bates, R.G., Pinching, G.D., 1949. Acidic dissociation constant of ammonium ion at 0 to 50 C, and the base strength of ammonia. J. Res. Natl. Bur. Stand. (1934). 42, 419–430. https://doi.org/10.6028/jres.042.037

Bello, M., Ranganathan, P., Brennan, F., 2017. Dynamic modelling of microalgae cultivation process in high rate algal wastewater pond. Algal Res. 24, 457–466. https://doi.org/10.1016/j.algal.2016.10.016

Benemann, J.R., 2008. Opportunities and challenges in algae biofuels production, in: Algae World 2008. Singapore, p. 15.

Benemann, J.R., 2003. Biofixation of CO2 and greenhouse gas abatement with microalgae—technology roadmap.

Bhavaraju, S.M., Russell, T.W.F., Blanch, H.W., 1978. The design of gas sparged devices for viscous liquid systems. AIChE J. 24, 454–466. https://doi.org/10.1002/aic.690240310

Bordel, S., Guieysse, B., Muñoz, R., 2009. Mechanistic model for the reclamation of industrial

wastewaters using algal– bacterial photobioreactors. Environ. Sci. Technol. 43, 3200–3207. https://doi.org/10.1021/es802156e

Borowitzka, M.A., 1999. Commercial production of microalgae: ponds, tanks, tubes and fermenters. J. Biotechnol. 70, 313–321.

Briens, C., Piskorz, J., Berruti, F., 2008. Biomass valorization for fuel and chemicals production - A review. Int. J. Chem. React. Eng. 6, 1–49. https://doi.org/10.2202/1542-6580.1674

Buhr, H.O., Miller, S.B., 1983. A dynamic model of the high-rate algal-bacterial wastewater treatment pond. Water Res. 17, 29–37. https://doi.org/10.1016/0043-1354(83)90283-X

Chu, W., Gao, X., Sorooshian, S., 2011. Handling boundary constraints for particle swarm optimization in high-dimensional search space. Inf. Sci. (Ny). 181, 4569–4581. https://doi.org/10.1016/j.ins.2010.11.030

Clerc, M., Kennedy, J., 2002. The particle swarm-explosion, stability, and convergence in a multidimensional complex space. IEEE Trans. Evol. Comput. 6, 58–73. https://doi.org/10.1109/4235.985692

Conway, D., Van Garderen, E.A., Deryng, D., Dorling, S., Krueger, T., Landman, W., Lankford, B., Lebek, K., Osborn, T., Ringler, C., Thurlow, J., Zhu, T., Dalin, C., 2015. Climate and southern Africa's water-energy-food nexus. Nat. Clim. Chang. 5, 837–846. https://doi.org/10.1038/nclimate2735

Craggs, R., Sutherland, D., Campbell, H., 2012. Hectare-scale demonstration of high rate algal ponds for enhanced wastewater treatment and biofuel production. J. Appl. Phycol. 24, 329–337. https://doi.org/10.1007/s10811-012-9810-8

de Godos, I., Blanco, S., García-Encina, P.A., Becares, E., Muñoz, R., 2010. Influence of flue gas sparging on the performance of high rate algae ponds treating agro-industrial wastewaters. J. Hazard. Mater. 179, 1049–1054. https://doi.org/10.1016/j.jhazmat.2010.03.112

Deng, X., Fei, X., Li, Y., 2011. The effects of nutritional restriction on neutral lipid accumulation in *Chlamydomonas* and *Chlorella*. African J. Microbiol. Res. 5, 260–270.

Frank, M.J.W., Kuipers, J.A.M., van Swaaij, W.P.M., 1996. Diffusion coefficients and viscosities of CO2 + H2O, CO2 + CH3OH, NH3 + H2O, and NH3 + CH3OH liquid mixtures. J. Chem. Eng. Data 41, 297–302. https://doi.org/10.1021/je950157k

Fuentes, J.L., Garbayo, I., Cuaresma, M., Montero, Z., Gonzalez-del-Valle, M., Vílchez, C., 2016. Impact of microalgae-bacteria interactions on the production of algal biomass and associated

compounds. Mar. Drugs 14, 100. https://doi.org/10.3390/md14050100

Gaden, E.L., 1959. Fermentation process kinetics. J. Biochem. Microbiol. Technol. Eng. 1, 413–429.https://doi.org/10.1002/(SICI)1097-0290(20000320)67:6<629::AID-BIT2>3.0.CO;2-P

Gomez, J.A., Höffner, K., Barton, P.I., 2016. From sugars to biodiesel using microalgae and yeast. Green Chem. 18, 461–475. https://doi.org/10.1039/c5gc01843a

Heubeck, S., Craggs, R.J., Shilton, A., 2007. Influence of CO_2 scrubbing from biogas on the treatment performance of a high rate algal pond. Water Sci. Technol. 55, 193–200. https://doi.org/10.2166/wst.2007.358

Hoffmann, M., Marxen, K., Schulz, R., Vanselow, K.H., 2010. TFA and EPA productivities of *Nannochloropsis salina* influenced by temperature and nitrate stimuli in turbidostatic controlled experiments. Mar. Drugs 8, 2526–2545. https://doi.org/10.3390/md8092526

James, S.C., Janardhanam, V., Hanson, D.T., 2013. Simulating pH effects in an algal-growth hydrodynamics model. J. Phycol. 49, 608–615. https://doi.org/10.1111/jpy.12071

Jupsin, H., Praet, E., Vasel, J.L., 2003. Dynamic mathematical model of high rate algal ponds (HRAP). Water Sci. Technol. 48, 197–204.

Kadam, K.L., 1997. Power plant flue gas as a source of CO_2 for microalgae cultivation: Economic impact of different process options. Energy Convers. Mgmt 38, S505–S510.

Kasiri, S., Ulrich, A., Prasad, V., 2015. Kinetic modeling and optimization of carbon dioxide fixation using microalgae cultivated in oil-sands process water. Chem. Eng. Sci. 137, 697–711. https://doi.org/10.1016/j.ces.2015.07.004

Leyva, L.A., Bashan, Y., Mendoza, A., De-Bashan, L.E., 2014. Accumulation fatty acids of in *Chlorella vulgaris* under heterotrophic conditions in relation to activity of acetyl-CoA carboxylase, temperature, and co-immobilization with *Azospirillum brasilense*. Naturwissenschaften 101, 819–830. https://doi.org/10.1007/s00114-014-1223-x

Li, Y., Zhou, W., Hu, B., Min, M., Chen, P., Ruan, R.R., 2012. Effect of light intensity on algal biomass accumulation and biodiesel production for mixotrophic strains *Chlorella kessleri* and *Chlorella protothecoide* cultivated in highly concentrated municipal wastewater. Biotechnol. Bioeng. 109, 2222–2229. https://doi.org/10.1002/bit.24491

Loewenthal, R.E., Marais, G. v. R., 1976. Carbonate chemistry of aquatic systems: Theory & application. Ann Arbor Science, Ann Arbor.

Luedeking, R., Piret, E.L., 1959. A kinetic study of the lactic acid fermentation. Batch process at controllet pH. J. Biochem. Microbiol. Technol. Eng. 1, 393–412. https://doi.org/10.1002/jbmte.390010406

Merchuk, J.C., Garcia-Camacho, F., Molina-Grima, E., 2007. Photobioreactor design and fluid dynamics. Chem. Biochem. Eng. Q. 21, 345–355.

Moreno-Garrido, I., 2008. Microalgae immobilization: Current techniques and uses. Bioresour. Technol. 99, 3949–3964. https://doi.org/10.1016/J.BIORTECH.2007.05.040

Mulbry, W., Kondrad, S., Pizarro, C., Kebede-Westhead, E., 2008. Treatment of dairy manure effluent using freshwater algae: Algal productivity and recovery of manure nutrients using pilot-scale algal turf scrubbers. Bioresour. Technol. 99, 8137–8142. https://doi.org/10.1016/j.biortech.2008.03.073

Muñoz, R., Guieysse, B., 2006. Algal-bacterial processes for the treatment of hazardous contaminants: A review. Water Res. 40, 2799–2815. https://doi.org/10.1016/j.watres.2006.06.011

Oswald, W.J., Gotaas, H.B., Golueke, C.G., Kellen, W.R., 1957. Algae in waste treatment [with discussion]. Sewage Ind. Waste. 29, 437–457.

Packer, A., Li, Y., Andersen, T., Hu, Q., Kuang, Y., Sommerfeld, M., 2011. Growth and neutral lipid synthesis in green microalgae: A mathematical model. Bioresour. Technol. 102, 111–117. https://doi.org/10.1016/j.biortech.2010.06.029

Panwar, N.L., Kaushik, S.C., Kothari, S., 2011. Role of renewable energy sources in environmental protection: A review. Renew. Sustain. Energy Rev. 15, 1513–1524. https://doi.org/10.1016/j.rser.2010.11.037

Park, J.B.K., Craggs, R.J., 2010. Wastewater treatment and algal production in high rate algal ponds with carbon dioxide addition. Water Sci. Technol. 61, 633–639. https://doi.org/10.2166/wst.2010.951

Park, J.B.K., Craggs, R.J., Shilton, A.N., 2011. Wastewater treatment high rate algal ponds for biofuel production. Bioresour. Technol. 102, 35–42. https://doi.org/10.1016/j.biortech.2010.06.158

Pereira, L.M.C., Chapoy, A., Burgass, R., Oliveira, M.B., Coutinho, J.A.P., Tohidi, B., 2016. Study of the impact of high temperatures and pressures on the equilibrium densities and interfacial tension of the carbon dioxide/water system. J. Chem. Thermodyn. 93, 404–415.

https://doi.org/10.1016/j.jct.2015.05.005

Posten, C., 2009. Design principles of photo-bioreactors for cultivation of microalgae. Eng. Life Sci. 9, 165–177. https://doi.org/10.1002/elsc.200900003

Ramanan, R., Kim, B.H., Cho, D.H., Oh, H.M., Kim, H.S., 2016. Algae-bacteria interactions: Evolution, ecology and emerging applications. Biotechnol. Adv. 34, 14–29. https://doi.org/10.1016/j.biotechadv.2015.12.003

Rawat, I., Ranjith Kumar, R., Mutanda, T., Bux, F., 2011. Dual role of microalgae: Phycoremediation of domestic wastewater and biomass production for sustainable biofuels production. Appl. Energy 88, 3411–3424. https://doi.org/10.1016/j.apenergy.2010.11.025

Reid, R.C., Prausnitz, J.M., Poling, B.E., 1987. The properties of gases and liquids. McGraw-Hill, New York.

Riekhof, W.R., Sears, B.B., Benning, C., 2005. Annotation of genes involved in glycerolipid biosynthesis in *Chlamydomonas reinhardtii*: discovery of the betaine lipid synthase BTA1Cr. Eukaryot. Cell 4, 242–252.

Ryu, B.G., Kim, J., Han, J.I., Yang, J.W., 2017. Feasibility of using a microalgal-bacterial consortium for treatment of toxic coke wastewater with concomitant production of microbial lipids. Bioresour. Technol. 225, 58–66. https://doi.org/10.1016/j.biortech.2016.11.029

Sah, L., Rousseau, D.P.L., Hooijmans, C.M., 2012. Numerical modelling of waste stabilization ponds: Where do we stand? Water, Air, Soil Pollut. 223, 3155–3171. https://doi.org/10.1007/s11270-012-1098-4

Salama, E.S., Kurade, M.B., Abou-Shanab, R.A.I., El-Dalatony, M.M., Yang, I.-S., Min, B., Jeon, B.-H., 2017. Recent progress in microalgal biomass production coupled with wastewater treatment for biofuel generation. Renew. Sustain. Energy Rev. 79, 1189–1211. https://doi.org/10.1016/j.rser.2017.05.091

Shang, H., Scott, J.A., Shepherd, S.H., Ross, G.M., 2010. A dynamic thermal model for heating microalgae incubator ponds using off-gas. Chem. Eng. Sci. 65, 4591–4597. https://doi.org/10.1016/j.ces.2010.04.042

Shilton, A.N., Mara, D.D., Craggs, R., Powell, N., 2008. Solar-powered aeration and disinfection, anaerobic co-digestion, biological CO2 scrubbing and biofuel production: the energy and carbon management opportunities of waste stabilisation ponds. Water Sci. Technol. 58, 253–258. https://doi.org/10.2166/wst.2008.666

Singh, J., Gu, S., 2010. Commercialization potential of microalgae for biofuels production. Renew. Sustain. Energy Rev. 14, 2596–2610. https://doi.org/10.1016/j.rser.2010.06.014

Solimeno, A., Samsó, R., Uggetti, E., Sialve, B., Steyer, J.P., Gabarró, A., García, J., 2015. New mechanistic model to simulate microalgae growth. Algal Res. 12, 350–358. https://doi.org/10.1016/j.algal.2015.09.008

Surendhiran, D., Vijay, M., Sivaprakash, B., Sirajunnisa, A., 2015. Kinetic modeling of microalgal growth and lipid synthesis for biodiesel production. 3 Biotech 5, 663–669. https://doi.org/10.1007/s13205-014-0264-3

Sutherland, D.L., Howard-Williams, C., Turnbull, M.H., Broady, P.A., Craggs, R.J., 2015. Enhancing microalgal photosynthesis and productivity in wastewater treatment high rate algal ponds for biofuel production. Bioresour. Technol. 184, 222–229. https://doi.org/10.1016/j.biortech.2014.10.074

Teplitski, M., Rajamani, S., 2011. Signal and nutrient exchange in the interactions between soil algae and bacteria, in: Witzany, G. (Ed.), Biocommunication in Soil Microorganisms. Springer, Berlin, Germany, pp. 413–426.

Tevatia, R., Demirel, Y., Blum, P., 2012. Kinetic modeling of photoautotropic growth and neutral lipid accumulation in terms of ammonium concentration in *Chlamydomonas reinhardtii*. Bioresour. Technol. 119, 419–424. https://doi.org/10.1016/j.biortech.2012.05.124

Wang, Z.T., Ullrich, N., Joo, S., Waffenschmidt, S. Goodenough, U., 2009. Algal lipid bodies: stress induction, purification, and biochemical characterization in wild-type and starchless *Chlamydomonas reinhardtii*. Eukaryot. Cell 8, 1856–1868.

Weyer, K.M., Bush, D.R., Darzins, A., Willson, B.D., 2010. Theoretical maximum algal oil production. Bioenergy Res. 3, 204–213. https://doi.org/10.1007/s12155-009-9046-x

Work, V.H., Radakovits, R., Jinkerson, R.E., Meuser, J.E., Elliott, L.G., Vinyard, D.J., Laurens, L.M.L., Dismukes, G.C., Posewitz, M.C., 2010. Increased lipid accumulation in the *Chlamydomonas reinhardtii sta7-10* starchless isoamylase mutant and increased carbohydrate synthesis in complemented strains. Eukaryot. Cell 9, 1251–1261. https://doi.org/10.1128/EC.00075-10

Yang, A., 2011. Modeling and evaluation of CO2 supply and utilization in algal ponds. Ind. Eng. Chem. Res. 50, 11181–11192.

Yang, J., Rasa, E., Tantayotai, P., Scow, K.M., Yuan, H., Hristova, K.R., 2011a. Mathematical

model of *Chlorella minutissima* UTEX2341 growth and lipid production under photoheterotrophic fermentation conditions. Bioresour. Technol. 102, 3077–3082. https://doi.org/10.1016/j.biortech.2010.10.049

Zhang, L., Shoji, M., 2001. Aperiodic bubble formation from a submerged orifice. Chem. Eng. Sci. 56, 5371–5381.

Zhang, W.-J., Xie, X.-F., Bi, D.-C., 2004. Handling boundary constraints for numerical optimization by particle swarm flying in periodic search space, in: Evolutionary Computation, CEC 2004. IEEE, Oregan, USA, pp. 2307–2311. https://doi.org/10.1109/CEC.2004.1331185